



# This is to certify that the

# thesis entitled

A Geochemical and Hydrological Investigation of a Modern Coastal Marine Sabkha

presented by

Robert Gudramovics

has been accepted towards fulfillment of the requirements for

Masters degree in Geology

Major professor

Date June 4, 1981

**O**-7639



OVERDUE FINES: 25¢ per day per item

RETURNING LIBRARY MATERIALS:
Place in book return to remove charge from circulation records

JAN 0 1 8 2004

# A GEOCHEMICAL AND HYDROLOGICAL INVESTIGATION OF A MODERN COASTAL MARINE SABKHA

bу

Robert Gudramovics

# A THESIS

Submitted to

Michigan State University

in partial fulfillment of the requirements

for the degree of

MASTER OF SCIENCE

Department of Geology

#### ABSTRACT

A GEOCHEMICAL AND HYDROLOGICAL INVESTIGATION OF A MODERN COASTAL

MARINE SABKHA

by

# Robert Gudramovics

The purpose of this study is to integrate the geochemistry and hydrology of a modern marine coastal sabkha and by doing so determine the origin and evolution of the subsurface brines. The study area is the Laguna Madre Tidal Flats, located approximately 90 km south of Corpus Christi, Texas.

The conclusions of this study are: 1) the major subsurface brine is a Na-Cl solution that is marine in origin and depleted in calcium with respect to sea water; 2) a second water mass, continental in origin, has been observed at depth toward the continental side of the tidal flats; 3) input of water to the sabkha is by the process of Flood Recharge during which the Laguna Madre waters are driven across the surface of the sabkha by high winds; 4) recharge area is selective and is a function of wind direction, wind velocity, and topography; 5) both water masses evolved chemically by the process of Evaporative Concentration with some subsequent precipitation of calcium carbonate and calcium sulfate minerals.

#### **ACKNOWLE DGEMENTS**

I would like to thank my committee members Dr. David Long, Dr. Graham Larson, and Dr. John Wilband who were helpful in the development and completion of this thesis. I would like to especially thank Dave who, in addition to being a very helpful advisor, became a needed friend. We endured broken vehicles, scorpions, black widows, hurricane Allen and the temperature extremes of the study area, and I endured his fiddle playing; from all of this we learned never to say "it can't get worse.

I would like to thank the United States Geological Survey in Corpus Christi for providing me with a research assistantship for this study. I would also like to thank Steve, Mark, Tom and all the other people from the "Chateau" who provided friendship to the "loud" New Yorker. I would especially thank my sister Rita and her husband Steve who provided a place in which to escape from all of this madness.

# TABLE OF CONTENTS

	page
LIST OF TABLES	v
LIST OF FIGURES	vi
INTRODUCTION	1
LAGUNA MADRE TIDAL FLATS	7
GEOLOGIC HISTORY	7
REGIONAL SETTING	9
SEDIMENT TYPE AND SOURCE REGIONS	12
CLIMATE	15
FIELD OBSERVATIONS	17
FIELD METHODS	20
ESTABLISHMENT OF WELL SITES	20
SAMPLING AND FIELD ANALYSES	23
GEOCHEMISTRY/HYDROLOGY	25
LABORATORY METHODS	29
GEOCHEMISTRY	33
EVAPORATIVE CONCENTRATION	33
SOLUTE FRACTIONATION	36
BRINE MIXING	38
OBSERVATIONS	40
DISCUSSION	47
HYDROLOGY	
SEEPAGE REFLUX	55

		page
	CAPILLARY ACTION	56
	EVAPORATIVE PUMPING	56
	FLOOD RECHARGE	58
	OBSERVATIONS	60
	DISCUSSION	66
BASI	N AREA	69
СОМР	UTER MODELING	73
SUMM	ARY AND CONCLUSIONS	83
BIBLIOGRAPHY 85		85
APPE	NDICES	91
	SULFATE ANALYSIS	91
	BROMIDE ANALYSIS	93
	DENSITY MEASUREMENTS	96
	ANALYSES	103
	HYDROLOGY	106

# LIST OF TABLES

Table		page
1.	Precision of Geochemical Analyses.	32
2.	Molar Ratios	49
3.	Key to letters used in Figure 8	51
4.	Selected chemistries for the basin brines as a	
	function of distance from gas well access channel.	70
5•	Mineral Saturation States	78
6.	Laboratory Density Measurements	102

# LIST OF FIGURES

Figure		Page
1.	Map of General Region	10
2.	Map of Sedimentary Provinces	13
3.	Map of Study Area	21
4.	Concentration Trends of Ions in Sea Water	35
5.	August Data	42
6.	August Data	43
7.	March Data	44
8.	March Data	45
9.	Trilinear plot of the Sample Waters	52
10.	Concentration Trends of Samples	53
11.	Reflux and Evaporative Pumping Models	57
12.	August Piezometric Potentials	63
13.	March Piezometric Potentials	64
14.	Basin Area August Piezometric Potentials	65
15.	Bromide Contour Maps	68
16.	Bromide vs. Transmittance	95
17.	Density vs. Temperature	99
18.	Density vs. Salinity	100
19.	Density vs. Temperature vs. Salinity	101

#### INTRODUCTION

Geochemical and hydrological processes in ancient sabkha systems have been proposed for the generation of: a) certain evaporitic minerals (Kinsman, 1969), b) various stratiform metalliferous deposits (Renfro, 1974), and c) low temperature uranium deposits (Rawson, 1976). A better understanding of these processes and their controls will advance our knowledge about these systems and also aid us in the exploration for these ancient mineral deposits. This study will test two hypothesis: a) that evaporative pumping (Hsu and Siegenthaler, 1969) is the major hydrological mechanism, and b) that evaporative concentration (Carpenter, 1978) is the dominant geochemical process operating in an active coastal sabkha. The study area is the Wind Tidal Flat area of Laguna Madre, which lies approximately 90 km south of Corpus Christi, Texas (Fig. 1).

Coastal sabkhas are flat (less than a 1/1000 seaward slope), salt encrusted, highly evaporitic environments which are occasionally inundated by flood waters (Kinsman, 1969). Due to their limited accessibility and inhospitable nature, only a few sabkhas have been studied in any detail in terms of the geochemical and hydrological processes effecting the associated brines. Framework sediments of coastal sabkhas may range from almost pure carbonate to noncarbonate, depending on local supply of terrigeneous detritus (Kinsman, 1969).

Sabkhas have been recognized as an active environment for the

precipitation of aragonite, gypsum, halite, dolomite, and various other evaporitic minerals only within the last two decades. The first sabkhas identified were located along the Persial Gulf, and therefore, are the type localities. These include the Abu Dhabi coastal sabkha, various coastal and continental sabkhas of the Trucial Coast, and the coastal sabkhas of the Qatar peninsula. These coastal sabkhas are predominatnly carbonate, while the continental sabkhas are characteristically composed of noncarbonate sediments (fine to medium-grained quartz).

The initial studies of the Persian Gulf sabkhas have dealt with general physiography, sedimentology, stratigraphy, fauna and geologic development Shearman, 1963; Kinsman, 1964,1966; Evans and Shearman, 1964; Illing et al., 1965; Evans et al., 1973). Later studies entailed the determination of the geochemisty and origin of the brines. From this various authors have proposed hydrological and geochemical models for the source and evolution of the brines, and the formation of the observed evaporitic minerals. Traditionally these models were based on the geochemcial variation of the brines, types of evaporitic minerals present, and the zonation of these evaporitic minerals (Kinsman, 1966; 1969; Friedman and Sanders, 1967; Butler, 1969; de Groot, 1973; Bush, 1973).

These early studies did not consider the climatological, sedimentological and geomorphological parameters that influence both the geochemisty and hydrology of the sabkha. The early investigations of the Abu Dhavi sabkha did comment on the very prominent "shamal" winds in the region but failed to integrate this climatological parameter with controls on the geochemical and

hydrological processes of this system. It seems that traditionally the major emphasis for understanding the processes operating within the sabkhas was that this was the only known environment where dolomite formed in situ (de Groot, 1973). Therefore, the main rationale behind hypothesizing hydrological and geochemical models for sabkhas was in the development of mechanisms to explain dolomite formation.

Additional coastal and continental sabkhas have since been identified and studies. A quartz sand-based coastal marine sabkha located in Baja California was studied by Phleger (1969). He investigated the distribution of evaporitic mineral on the surface of the sabkha. In addition he observed that periodic flooding of the area by marine water driven onto the surface of the sabkha by winds could produce the observed distribution of these minerals. Phleger (1969) attributed the formation of these minerals and the origin of the brines to a flood recharge hydrological process. In the Bardawil coastal plain, northern Sinai, Levy (1977a,b) studied a quartz sand-based coastal marine sabkha. In this study two distinct water masses were observed within the sabkha. A NaCl and a CaCl2 brine, both of which he attributed to a normal marine parent. Levy (1977a,b) points out that these brines are distinct because of the different geochemical processes effecting them. The NaCl brine was generated by evaporative concentration and subsequent solute fractionation of a marine water, while the CaCl<sub>2</sub> brine was generated by solute fractionation, of the NaCl brine, as a result of the brine interacting with evaporitic minerals present within the sabkha. West and others (1979) investigated the presence of gypsum

nodules in a modern sabkha on the Mediterranean coast of Egypt. The sabkha was carbonate based and the origin of the brine within it were not determined, however West and others (1979) state that the brines are not solely sea water derived. Their investigation attributed the origin of the gypsum nodules to sulfate rich hypersaline groundwater (60°/oo) dissolving gypsum crystals below the water table and reprecipitating near the surface because of evaporation of this water. Migration is upward by capillary movement. Rouse and Sherif (1980) investigated the origin of brines along a quartz sand-based coastal marine sabkha along the Gulf of Sirte, Libya. A sulfur isotope analysis revealed that a major source of the brines is contenental water, and only by occasional flooding during the winter months does a minor amount of marine water enter the system.

A major weakness of these past works was that none have integrated both a detailed hydrological and geochemical investigation of an active coastal sabkha. It has only been recently that this type of investigation of a modern coastal marine sabkha has been conducted. McKenzie and others (1980) investigated the Abu Dhabi sabkha, in the Persian Gulf. In this study an isotope analysis of oxygen and hydrogen was conducted to determine the origin of the brines and the hydrological mechanism operating in the area. Three distinct zones, based on brine composition, were observed, each having a distinct hydrological mechanism operating within them. The area of the sabkha subject to periodic flooding, near the coast, had flood recharge of marine derived water as the major hydrological process occurring. Toward the continent, in an area with occasional flooding, a zone of mixed waters exists. These waters are a mixture

of a marine and a continentally derived water. In this zone a transitory hydrostatic state (McKenzie et al., 1980) exist, which is a function of the amount of flooding. Immediately after flooding this zone exhibits a flood recharge hydrostatic state; afterwards capillary action occurs and when flooding has not occurred for an extended period, evaporative pumping becomes the major hydrologic process. In the zone closest to the continent evaporative pumping of continentally derived waters is the dominant hydrological mechanism. This study demonstrated that the hydrology and geochemisty of the system are controlled by the climatological, stratigraphical and geomorphological parameter of the area.

The major hydrological models that have been proposed in the past for sabkhas are: a) Reflux (Adams and Rhodes, 1960), b)

Capillary action (Friedman and Sanders, 1967), c) Flood recharge (Butler, 1969), and d) Evaporative pumping (Hsu and Siegenthaler, 1969). The geochemcial models based on the behavior of ions within the interstitial waters are: a) Brine mixing (Raup, 1970), b) Evaporative concentration with subsequent solute fractionation (Carpenter, 1978), and c) Solute fractionation as a result of the interaction of brines with host sediment and/or present evaporitic minerals (Eugster and Jones, 1979).

The geochemical and hydrological investigation of the Laguna Madre sabkha was initiated with the establishment of a well system in the area (Fig. 3) during July, 1979. Water depths were measured at each well site and water samples for chemical analysis were taken from each well, as well as from the trench dug at each well site, the Intracoastal Waterway, and the gas access canals. The data for this

study was obtained from two field expeditions, August, 1979 and March, 1980. The hydrology of the system was determined from the piezometric potentials of the interstitial waters as a function of locality and depth. The geochemisty of the waters was determined by the analysis of the major ions in the water samples obtained during each sample period. Previous studies of the Wind Tidal Flat of Laguna Madre include a sedimentological and stratigraphical study conducted by Fisk (1959), as well as a preliminary hydrological and geochemical investigation of the sabkha conducted by Amdurer (1978). The latter investigation, however, was limited to the number of well sites established to accurately define this system.

Geologic systems are rarely simple or identical; each is unique because of the various minor or major factors effecting it. This study will further refine our knowledge about coastal sabkha systems. The Abu Dhabi sabkha has been extensively studies and we now have a thorough understanding of one system (McKenzie et al., 1980). This study will determine the geochemical and hydrological processes operating within the Laguna Madre sabkha and how the climatological, sedimentological and geomorphological parameters of this area effect it. In doing so one can determine some common processes occurring in coastal sabkhas and what parameters effect them. By doing this one will be better able to evaluate which of these processes can have occurred in ancient sabkhas and determine if and how they generated ore deposits.

#### LAGUNA MADRE TIDAL FLATS

# Geologic History

A combination of factors have led to the origin and development of the Laguna Madre tidal flats. These include fluctuations in sea level, regional uplift, climatic conditions, and the amount and type of sediment input into the flats by streams and longshore currents.

During the early Pleistocene the southern Gulf coastal region was a relatively stable barrier island and back lagoonal coastal plain (Price, 1933). The mainland margin north of the Rio Grande was the original shoreline, as indicated by the presence of deltaic, lagoonal and barrier island features in the coastal plain (Price, 1958). The development of major continental glaciers during the Wisconsinan ice age resulted in lowering of sea level by approximately 140 meters and subsequent migration of the shoreline 80 to 230 kilometers gulfward (LeBlanc and Hodgson, 1959). Streams then cut into the exposed Pleistocene surface and barrier islands formed gulfward of the new coastline. Stream valleys up to 38 meters in depth have been measured beneath the tidal flats (Fisk, 1959; Wilkinson, 1975).

As the glaciers began to melt at the end of the Wisconsinan ice age a steady rise began in sea level accompanied by coastline and barrier island transgression. Sea level first rose at a rapid rate

until approximately 4000 years ago when the rate of rise decreased sharply (Amdurer et al., 1979). Post-Pleistocene regional uplift of approximately a meter along the gulf coast also occurred (Price, 1933, 1947; LeBlanc and Hodgson, 1959; Fisk, 1959). This raised the gulf coastal plain sufficiently to develop the existing Texas coast and barrier island chain gulfward of its Pleistocene counterpart. About 6000 years ago when sea level reached within 7.5 - 9.0 meters of its present level the divides between the estuaries and bays were flooded and the group of widely separated barrier islands began to grow (Amdurer, 1978).

Quaternary sediments which accumulated in estuarine, lagoonal and eolian environments, overlie the erosional surface of the Pleistocene sediments in the area. Sedimentation continued at a rate of approximately 3.1 meters per thousand years until, about 4000 years ago, the separated islands merged to form a continuous barrier island and an extensive lagoon west of the barrier islands resulted (Amdurer et al., 1979). A sedimentation rate of 1 meter every 150 years has been recorded in situ by Fisk (1959), and indicates that the final closing of the Laguna Madre depression at the western edge of the Sand Bulge occurred approximately 150 years ago (Price, 1958; Fisk, 1959). Presently the Laguna Madre tidal flats are still being modified by extensive winds in the area. Sedimentation and deflation occur continuously by eolian processes; also, occasional storms temporarily open passes on Padre Island. Therefore, the surficial features of the Laguna Madre are constantly reequilibrating.

# Regional Setting

The Laguna Madre tidal flat is located approximately 90 km south of Corpus Christi, Texas. Situated along the Gulf of Mexico coastline it is 22 km in width, 26 km in length and has a total area greater than  $550 \text{ km}^2$ . The tidal flat is bordered on the west by a remnant Pleistocene eolian coastal plain and on the east by a barrier island.

Padre Island (Fig. 1) is one of the major islands which make up the Texas coast barrier—island chain. It extends from just south of Corpus Christi Bay to the Brazos Santiago Pass which is just north of Mexico, a distance greater than 180 km. It extends almost parallel to the Texas coast and forms slightly gulfward arc at its southern end.

The Laguna Madre itself is divided into two halves by the Laguna Madre tidal flat, each half is restricted by a mud flat which further separates the lagoon. The northern Laguna Madre is separated into two distinct basins by the "Middle Ground", a mud flat that is about 3.2 km in length and located midway between the tidal flat and Baffin Bay. The more northern basin extends 64 km north of the Middle Ground and has a depth of less than 1.5 m. The southern basin of the northern Laguna Madre is called "The Hole". Its dimensions are 16 km in length, 3.2 km in width and has an average depth of 1.5 m.

The southern Laguna Madre has a greater width than its northern counterpart. The southern lagoon is constricted by a mud flat that is located opposite the Arrayo Colorado. The more northern part is called Red Fish Bay, which has a maximum width of 9.7 km and an average depth of less than 3 m. It shoals to a depth of less than 1 m at the location where it curves westward into the tidal flat. The

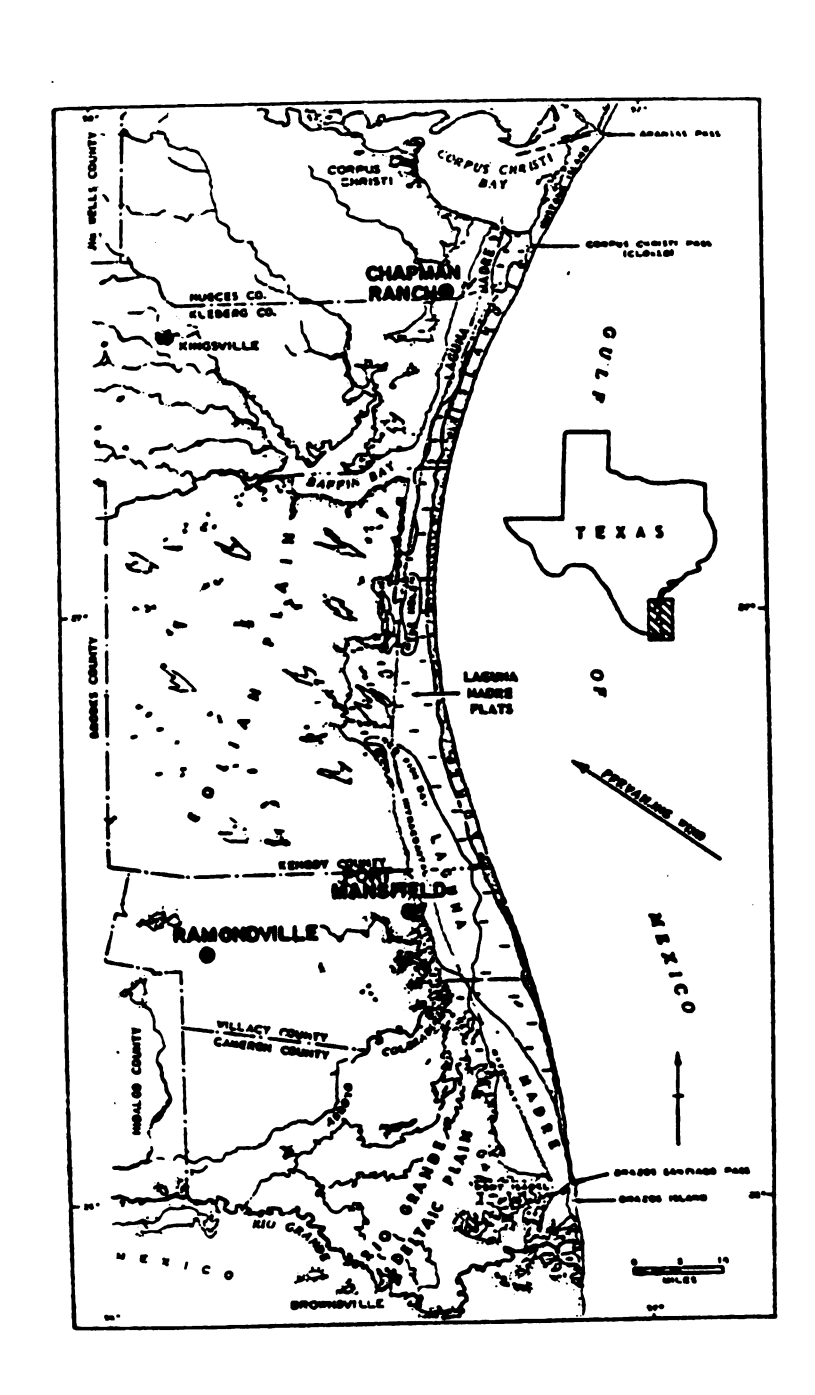


Figure 1. Map of general area (after Fisk, 1959)

more southern half has a length of 40 km, a width of 11 km and a depth of approximately 1.5 m.

In 1949 an Intracoastal Waterway (ICWW) was dug through the Laguna Madre. This ship channel is 6.5 m wide and 3.7 m deep. Additional canals have since been dug within the flats (Fig. 3). These canals are used for gas well access and are usually less than 3.5 m in width and 2.1 m in depth. Due to the length of Padre Island, the nearest sea water input to the Laguna Madre are at Aransas Pass, 108 km north of the tidal flats and at Brazos Santiago Pass 87 km south of the flats. Therefore, the lagoonal waters, even though they are derived from the Gulf of Mexico, were chemically distinct because they can be modified by rain, river input, and/or high degrees of evaporation. For example, a minimum of 12.5 % on and a maximum of 108.6 % oo have been measured for the surface waters of the lagoon (Fisk, 1959).

The Laguna Madre tidal flats merge to the east with the hummocks and dunes of Padre Island and to the west with an erosional reentrant of the mainland margin (Fisk, 1959). A few islands consisting of mainland remnants also exist within the western section. The largest of these are the Mesquite Rincon and El Toro. The Basin (Fig. 3) is a topographically low region of the flats, which often had ponded water prior to the construction of the Intracoastal Waterway. The boundary of it is characerized by low topography and surface sediment consisting of soft, spongy gypsiferous clays (Fisk, 1959). The Sand Bulge is another prominent feature of the flats. This area extends west from Padre Island and is characteristically higher in elevation than the rest of the flats and is composed of loose sands low in mud content.

# Sediment Type and Source Regions

The Laguna Madre tidal flats consists predominantly of sand, with minor amounts of clays, gypsum, and algal micrite. The sand composition is approximately 90 percent quartz with feldspar, chert, shell fragments and heavy minerals comprising the remaining 10 percent (Amdurer, 1978). Clay composition is predominantly illite with minor amounts of fine grained quartz and calcite (Fisk, 1959). Sands from beach, barrier island, dune, tidal flat and washover fans are subangular, sorted to well sorted, and fine to very fine grained. Sediment samples from these regions have varying amounts of clays. Textural and compositional uniformity of these sands indicate a similar source region (Amdurer, 1978).

Five depositional provinces have been defined for the northern Gulf of Mexico; a) Eastern Gulf, b) Mississippi, c) Western Gulf, d) Rio Grande and e) Texas Coast (Van Andel and Poole, 1960). Each is characterized by the heavy-mineral suite within the sediment. They are defined by the rivers providing the sediment to the Gulf and by the region in which this sediment is depositied. Two suites of heavy minerals have been identified within the Laguna Madre flats (Fig. 2)(Van Andel and Poole, 1960). The northwest corner of the tidal flat is characterized by heavy minerals consisting of tournaline, zircon, kyanite and stauralite. This suite of minerals originated from the Colorado, Brazos and other central Texas rivers, and therefore occur in the Western Gulf province. The sediment was transported to the tidal flat from the input areas by southerly longshore currents along the Gulf coast. A much larger portion of the tidal flat sediment

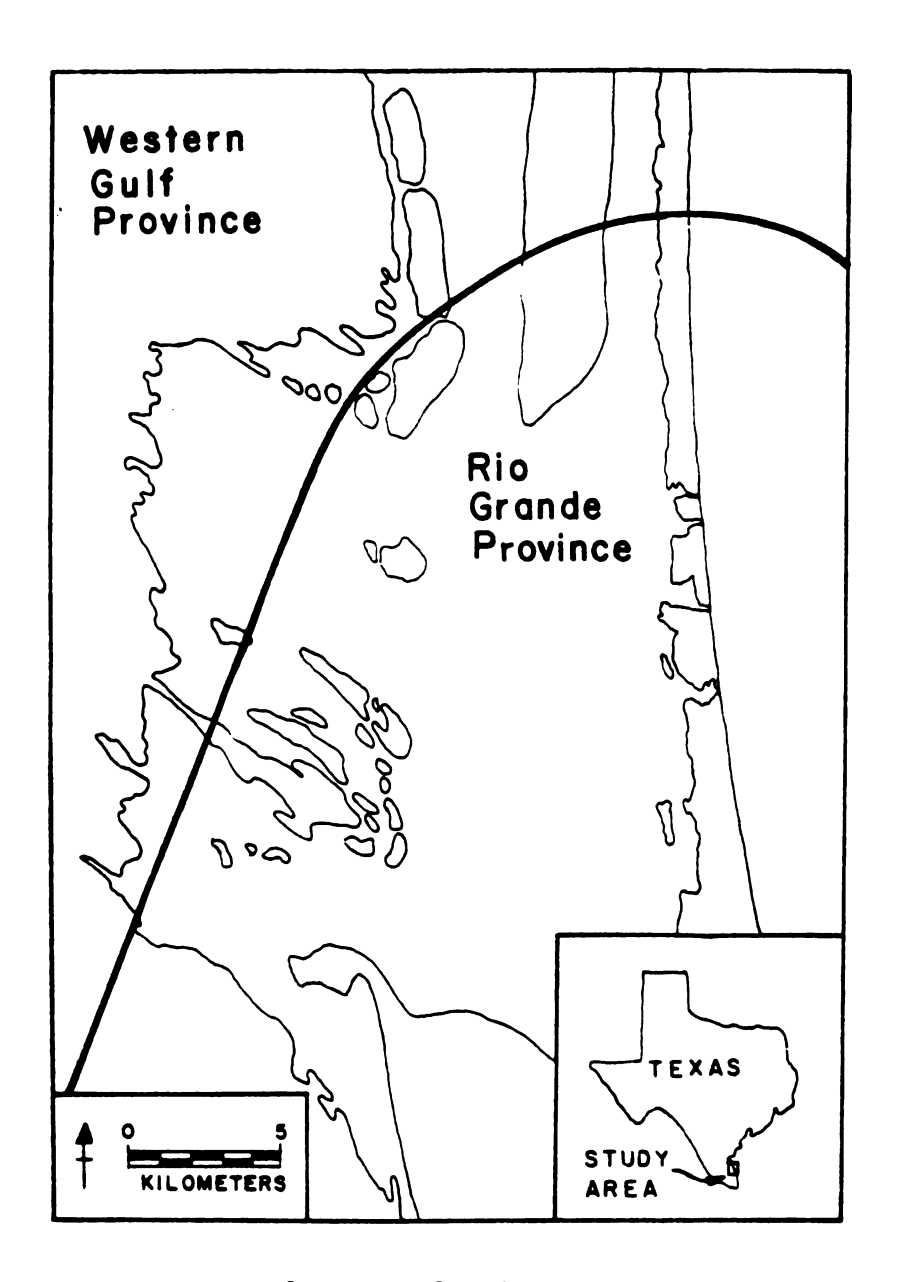


Figure 2. Map of sedimentary provinces.

contains green hornblende, pyroxenes (mostly augite), epidote and basaltic hornblende. This suite is characteristic of the Rio Grande province. A clay assemblage consisting of illite also indicates a Rio Grande source (Fisk, 1959). Evidently, the sediment of this province is transported to the Gulf of Mexico from the Rio Grande. This sediment as well as older reworked sediment located on the continental shelf and deposited during a lower sea level are then transported to the tidal flat by northerly longshore currents and deposited on Padre Island. The sediment is then transported to the flats by the dominant southeasterly winds of the area.

Heavy mineral composition of sediment in Laguna Madre indicates two source regions for this terrigenous sediment. Central Texas rivers evidently provide sediment to the northwest region of the flats, but the major portion of the flats appear to have a Rio Grande sediment source region. Although there are two sedimentary provinces defined in the Laguna Madre tidal flats, all sediments within the study area are relatively uniform in texture and composition. The reasons for this are that both the central Texas rivers and the Rio Grande drain similar regions, both provinces have sedimentary input into the Gulf at similar rates, and both provinces have similar processes of sediment transport and deposition. The major variations found in the sediment are therefore a function of the distance between the sediment locale and Padre island, and the energy of the environment of deposition.

## Climate

The climate in the coastal region of south central Texas is semi-arid (N.O.A.A., 1979). Climatological data for the Laguna Madre tidal flats is, however, lacking; therefore, the climate has been inferred for the area from five surrounding meteorological stations. These are: Corpus Christi, Chapman Ranch and Kingsville to the north, and Port Mansfield and Raymondville to the south (Fig. 1). All stations are located within 90 km of the study area.

Meteorological data from 1941 through 1970 indicates a normal yearly temperature of 22.6°C and a normal yearly precipitation of 70.0 cm (N.O.A.A., 1980). The normal summer temperature is 29.1°C and the precipitation is 6.1 cm. During May and September rainfall is greatest and during the winter months rainfall is the lowest. The period of June through November is the tropical storm season. this time almost all precipitation can be attributed to these storms. Summer sunshine exists for eighty percent of the possible time. The months of September and October experience a climate that is a continuation of summer conditions. Prevailing winds are from the southeast, resulting in relatively mild summer temperatures. Occasional shifts in wind direction result in temperatures rising above 38.0°C during the summer. Relative humidity averages 50 to 60 percent, with summer morning highs greater than 90 percent. During the present study, 28.5°C was the average 1979 summer temperature and 9.43 cm the average monthly summer precipitation; temperature highs reached 37.0°C. In 1980 the average summer temperature and monthly precipitation was 29.6°C and 8.36 cm

respectively, with a temperature high of 37.9°C. In July, 1979, the month prior to sampling, the average temperature and precipitation were 29.3°C and 7.37 cm respectively; while in August, 1979 the average temperature and precipitation were 29.1°C and 7.58 cm respectively. In February, 1980 average temperature and precipitation were 14.7°C and 3.16 cm respectively, and during the March, 1980 sampling period 19.6°C and 1.28 cm reflected the average temperature and precipitation.

During August 9-10, 1980 hurricane Allen struck the south Texas coast. During the period prior to Allen a severe drought and heat spell affected the area. Only 0.03 cm of precipitation fell. As a result of Allen, 24.9 cm of rain fell during a two day period. The high winds and rains produced extensive flooding. Other hurricanes that occurred in the past and their effects on the area are:

September, 1971, hurricane Ceila, 31 cm of rain; September, 1967, hurricane Beulah, 22 cm of rain in one day.

One must note that even with these weather extremes the potential evapotranspiration rate of the area is 100 to 120 cm per year (Rusnak, 1960), while the annual precipitation rate is only 70.0 cm. This results in an annual average precipitation deficiency of 30 to 50 cm.

## Field Observations

In the period of March, 1979 to August, 1980, numerous field expeditions were undertaken to the Laguna Madre tidal flats. This study was initiated in March, 1979 with a reconnaissance expedition to the area. At that time the area was relatively dry and extensively covered with desiccated algal mats. During the period of June, 1979 through August, 1979, field logistics and establishment of well sites were completed. During August, 1979 and March, 1980, water samples were obtained from the well sites and from surficial water bodies.

At various times during the study period the tidal flats were flooded. This resulted from periods of intense rain, high winds and during and after hurricane Allen. Flooding also occurred in June, 1979 after a period of heavy spring rains and an aerial flight over the study area indicated that more than half of the tidal flats were covered with water. Standing water remained until the end of June and within a month of normal weather conditions, the once moist and extensive algal mats became desiccated. In March, 1980 during a five day sampling period, an extensive area between well site 13 and 12 (Fig. 3) was observed to undergo flooding. This was produced by the continuous high winds from the northwest which pushed waterway and canal waters onto the flats and spread them in a southeasterly direction. With the termination of these winds, flooding ceased on the following day and the once extensive flood sheet began to separate into numerous smaller ponds. At that time algal mats on the eastern side of the tidal flats were moist and extensive while those on the western side were dry and desiccated. In the summer of 1980 an

extensive drought with high temperatures affected the region. This produced extensively desiccated algal mats throughout the area and concurrently the waters of the Intracoastal Waterway and gas access canals became more brackish than normal for this time of year.

Effects of the hurricane on the area were extensive and widespread for the entire tidal flat was flooded and numerous storm passes were reopened on Padre island. Water depths varied as a function of local topography with greater than nine feet of water covering some areas. Full analysis of flood waters has yet to be done, however the salinity of the water was recorded and was found to be less than that of normal sea water. This suggests that a significant portion of the flood water originated as continental runoff. Standing water remained on the flats for more than one week, with topographically higher areas, such as the Padre Island side, draining faster than the lower areas, such as the basin. Two weeks after the hurricane struck, a trench was dug at well site 13 and a water table measurement indicated a near normal water depth. algal mats which had previously covered the study area were no longer present; instead rounded clasts of algal mats ripped up by the hurricane flood waters were found throughout the area. Wells protruded several additional inches from the ground indicating that some surficial sediment had been eroded.

Fresh selenite rosettes were observed within the sediment at various well sites on the western side. Depth of occurrence varied for each well site. These crystals were distinct from selenite crystals dredged during Intracoastal Waterway construction. Spoil mound ctystals averaged 10 cm in diameter with some crystals greater

than 1 m in diameter. These crystals contained varying amounts of impurities such as sand and shell fragments. A more detailed description of these crystals is given by Masson (1955). The selenite rosettes found at the well sites averaged 2 cm in diameter and contained little to no impurities. These crystals apparently are less mature than those found at the spoil mounds. In addition to the presence of gypsum rosettes, preliminary analysis of a few cores revealed fine grained crystals of iron sulfides.

In July, 1980, before hurricane Allen struck, a brief expedition to the northwest section of the tidal flats showed that the algal mats were widespread but were not present thorughout the northwest section for westward, beyond this boundary, a very white, sun-bleached sand covers the flats. Springs were also found. Apparently animals within the area dug shallow holes which then filled up with interstitial waters. This water tasted less brackish than normal sea water, indicating possible continental input of interstitial waters. Within the sand pile from the dug hole gypsum crystals were found. These crystals, however, were not similar to the characteristic selenite rosettes found at the well sites; instead they formed yellow-green, clear, euhedral crystal. This crystal morphology has been described by Kinsman (1966) as typical of anhydrite which has rehydrated to gypsum due to its contact with less saline, continental groundwater from inland areas. Analysis of these crystals and the groundwater within this area has to be completed before this interpretation can be properly evaluated.

#### FIELD METHODS

## Establishment of Well Sites

During the period of June, 1979 through August, 1979 seventeen well sites were established in the Laguna Madre tidal flats (well sites 2-18; Fig. 3). At each well site a 1.9 m, 3.0 m and a 3.8 m length of 5 cm in diameter PVC (polyvinylchloride) pipe was pounded into the sediment with a Divercoring apparatus. This device consists of a 5 cm inside diameter pipe sleeve which fits over the PVC tube, a shaft connected to the sleeve which is used to guide the hammer, and a 18 kg cylindrical hammer which fits onto the shaft and is used to pound the PVC tube into the sediment. With this device 3.8 m is the maximum length of tubing that can be inserted practically into the sediment. After it is inserted into the ground a 5 cm plug is used to provide an air tight seal for the 3.0 m PVC pipe. A clamp is then placed around the pipe to provide a grip; the pipe is then pulled from the ground.

Cores between 1.2 m and 2.1 m in length have been recovered with the coring device described above. Once out of the ground the pipe is then cut to the length of the sediment core, capped and sealed at both ends. The shallow and deep wells, 1.9 m and 3.8 m PVC tubes respectively, had the sediment removed from them with a modified hand auger. Additional augering was required for some wells because of

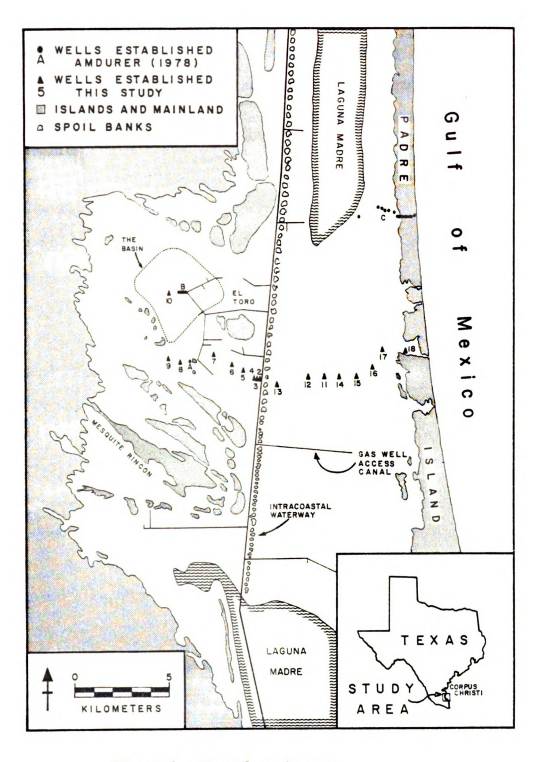


Figure 3. Map of study area

sediment oozing into them. Upon removal of sediment the wells are labeled and PVC caps are placed on them. These caps prevent rain water, flood water and sediment from entering the well. Once established, these wells (sites 2 through 18, Fig. 3) along with well site A and well set B (Fig. 3) were then accurately mapped. Surface elevation was then determined for each well site by the use of an Auto-leveler.

# Sampling and Field Analysis

There were two sampling periods during this present study,
August, 1979 and March, 1980. Water samples collected in August were
taken from the Intracoastal Waterway, a gas well access canal located
near well set B, well sites 2 through 18, well site A and well set B
(Fig. 3). Water samples collected in March were taken from: the
Intracoastal Waterway, gas well access canal located near well site A,
surficial flood waters between well sites 12 and 13, well sites 2
through 9, well sites 11 through 18, and well site A (Fig. 3). Well
site samples included trench water, and shallow and deep well waters.

The water sampling procedure required two visits to each well site. At the first visit, water depths were measured within the shallow and deep wells, a trench was dug and sampled, water table depth was measured within the trench, and the wells were pumped dry. On the second visit water samples were only taken from the shallow and deep wells.

To eliminate the possibility of water contamination a hand operated peristaltic pump with tygon tubing was used for the well sampling. Before the sample was collected distilled water was first run through the tygon tubing, followed by some well water. Each water sample was stored in a 500 ml and a 125 ml polyethylene bottle. Five milliliters of 70% formaldehyde was also added to the 125 ml bottle to suppress any organic activity. During sample collection, field analysis included temperature and pH determinations. Within 10 hours after the water samples were collected, alkalinity was determined by sulfuric acid titration (Brown et al., 1970). Alkalinity and

chlorinity determinations were not performed during sample collection because of equipment limitations.

# Geochemistry/Hydrology

Early investigations of the Laguna Madre Tidal Flats did not specifically deal with determining the geochemical and hydrological processes of this system; however, they do report on certain geochemical and hydrological characteristics of the area. Masson (1955) investigated the origin and distribution of gypsum within the Laguna Madre Tidal Flats. He found that selenite rosettes increase in size with depth. Masson also reports that flood waters on the surface of the tidal flats reach three times the concentration of sea water. From the distribution of the selenite crystals within the sediment, the analysis of this flood water, and the field observations of Laguna Madre waters being pushed onto the tidal flats, Masson (1955) postulates that the gypsum precipitates, within the sediment, from a highly saline water similar to sea water in composition. He states that the Laguna Madre waters are periodically moved as wind blown sheets across the surface of the tidal flats and then sink into the underlying sediment to provide a source for these highly saline brines.

A detailed investigation of the Laguna Madre Tidal Flats was conducted by Fisk (1959). This study dealt mainly with the geomorphology and geologic hyistory of the area; however, some geochemical analysis of surficial Laguna Madre waters and tidal flat interstitial waters were reported. From field observations of surface flooding, Fish (1959) postulates that the highly saline interstitial waters are recharged by flood waters. These flood waters are blown onto the tidal flats from the Laguna Madre and seep

downward. Fisk (1959) also points out that there is a high variability in Laguna Madre water salinity.

It has been only recently that a detailed geochemical and hydrological investigation of the Laguna Madre sabkha has been conducted. Amdurer (1978) postulates that reflux and evaporative concentration control the hydrological and geochemical processes, respectively. He suggests that the Laguna Madre waters are pushed onto the sabkha surface by high winds, but only at a few sites does this water seep downward. These localities are where the algal mats are desiccated and cannot prevent the water from flowing downward. This selective recharge, he states, leads to the low variability in brine composition relative to the high variability of the source This high variability of the source waters is attributed to these waters evaporating, becoming diluted by additional flood waters, and dilution by rain water. For the Sand Bulge area, Andurer (1978) postulates that reflux is occuring toward the Intracoastal Waterway. This is supported by the fact that for all his well sites the piezometric potential decreased with depth and the piezometric surface sloped toward the waterway. In addition, Amdurer (1978) suggests that the hydrology of the system was significantly changed with the introduction of the Intracoastal Waterway because it provides an escape route for the brines within the system.

Evaporative concentration of this flood water is the geochemical process occurring; however, because calcium is fractionated from the water by the precipitation of algal micrite, gypsum does not precipitate (Amdurer, 1978). Amdurer (1978) states that this is supported by thermodynamic modeling of the waters which indicate that

gypsum is undersaturated, and the lack of field evidence for gypsum occurring in situ.

During a preliminary field trip to the Wind Tidal Flats in March of 1979, fresh gypsum crystals were found in the area. This suggested that the geochemical processes postulated by Amdurer (1978) were not necessarily accurate for the entire system. His study was limited by the distribution of his well sites and their interaction with the fresh water lenses of nearby islands.

Well site A, well set B and well set C (Fig. 3) are the well sites established by Amdurer (1978) to define the sabkhas hydrology and geochemisty. From figure 3 one can see that well site A could be affected by the freshwater lens of the small nearby island (this has been found to be true during the present study). Well set B (Fig. 3) found within the "Basin" area of the tidal flats has been found to have a typical brine geochemistry and, therefore, would not be an accurate representation of the average brine geochemistry.

Well set C (Fig. 3) was used primarily by Amdurer (1978) to delineate sabkha hydrology and geochemistry. Except for the western most well, all the wells in well set C lie less than 1.5 km from Padre Island. Well site 17 (Fig. 3), established during this present study has been found to be influenced by the fresh water lens of Padre Island. Since well site 17 lies approximately 1.5 km from Padre Island this indicates that the wells used by Amdurer (1978) were similarly affected. In addition, Amdurer (1978) postulates a reflux of brine toward the Intracoastal Waterway; however, his western most well site is about 5 km from the geochemical and hydrological investigation of the Laguna Madre sabkha, the localities

and possible influences of the fresh water lenses of nearby islands influenced his geochemical and hydrological interpretations of the area.

This study was designed to avoid the limitations of the past work in the area. The distribution of the well sites and the well depths were determined in order to avoid the potential influences of the freshwater lenses of nearby islands and to obtain a complete cross section of piezometric potentials from well sites westward of the Intracoastal Waterway fo Padre Island. In doing so this study will accuately define the geochemical and hydrological processes that are occurring within the Laguna Madre sabkha.

## LABORATORY METHODS

Within 72 hours after collection in the field, the water samples were taken to a laboratory at Corpus Christi. The samples in the 500 ml bottles were filtered using a 0.45 micron membrane filter. Chlorinity was then determined by Mohr titration (Brown et al., 1970). After analysis the samples were acidified to a pH of less than 2.0, by adding concentrated HNO3. They were then packed and shipped to the geochemistry laboratory at Michigan State University for further analysis. The precision of the chemical analysis is shown in Table 1.

In Michigan, the 125 ml, formaldehyde treated samples were analysed for sulfate. Sulfate analysis was performed by a slightly modified technique proposed by Dunk et al. (1969) (Appendix A). The remainder of the analyses were done using the filtered and acidified water samples in the 500 ml bottles. Potassium analysis was conducted on 1/10 dilutions of Intracoastal Waterway and canal samples; for the other samples a 1/100 dilution was required. Standards and blank solutions contained 1000 mg/l sodium to suppress ionization of K during analysis by A.A. (atomic absorpion). Samples already contained at least this amount of sodium; therefore, addition of sodium to them was not necessary. Calcium analysis was conducted on 1/100 dilutions of all samples. After a 10 g/l lanthinum matrix was added to the samples and standards to suppress ionic interferences (particularly

from SO<sub>4</sub>) and ionization during A.A. analysis. This was accomplished by mixing 1 ml of 50 g/l lanthinum to 4 ml of sample and standards prior to aspiration in the A.A. A 10 g/l lanthinum blank was used in this analysis.

Sodium and magnesium analysis were performed on 1/1000 dilutions of samples. This dilution was necessary in order to have the Na and Mg concentrations of these samples within the measurable limits of the A.A. In addition, sodium analysis was conducted by Flame Emission with a rotated A.A. flame peak because of the high concentrations of Na in the samples. To suppress ionic interferences and ionization during both Na and Mg analysis a 10 g/l La matrix for both samples and standards was necessary. La was added to the samples during dilution.

Strontium was analysed on a 1/10 dilution of the samples. A 10 g/l chloride matrix was prepared for the standards and blank. This was necessary to minimize error due to variations in viscosity and vaporizing temperatures between samples, standards and blank during A. A. analysis.

Bromide analysis was performed colormetrically by a method used by Presely (1971). This method requires oxidizing the bromide with chloramine-T (sodium paratoluene-sulfonchloramine) and measuring the resultant color change spectrophotometrically at 595 millimic rons setting. This technique requires the use of bromide standards to generate a working curve for bromide concentrations and absorbance. The technique used has been modified from that proposed by Presely (1971) because of the greater Br concentrations encountered. A more detailed description of this procedure and modification is given in

## Appendix B.

Density measurements were done with the use of a pycnometer. Conversion of density values measured at laboratory temperatures to density values at field temperatures were required for the determination of the systems hydrology and use in the chemical modeling of the system by the WATEQ program (Truesdell and Jones, 1973). The conversion and formulas used are given in Appendix C.

Table 1

# Precision of Geochemical Analysis

Measurements	Precision
рН	<u>+</u> 0.04 units
Density	$\pm$ 0.0003 g/cm <sup>3</sup>
Alkalinity	<u>+</u> 6.0%
Br	<u>+</u> 1.8%
Ca	<u>+</u> 3.0%
C1	<u>+</u> 6.0%
K	<u>+</u> 3.0%
Mg	<u>+</u> 2.0%
Na	<u>+</u> 5.0%
S0 <sub>4</sub>	<u>+</u> 5.0%
Sr	<u>+</u> 3.0%

## **GEOCHEMISTRY**

Three geochemical mechanisms have been hypothesized for the chemical evolution of waters within sedimentary basins. These are:

a) evaporitic concentration (Carpenter, 1978), b) solute fractionation (Eugster and Jones, 1979), and c) brine mixing (Raup, 1970). This investigation will test the hypothesis that evaporitic concentration is the dominant geochemical mechanism effecting the brines within the Laguna Madre sabkha.

Evaporitic concentration - this mechanism attributes the behavior of solutes and the resultant chemical nature of the interstitial brines to the removal of water from that brine (Carpenter, 1978) by the process of evaporation. In evaporative concentration the ratios of ions within the solution remains constant until the onset of mineral precipitation. The constant relationship between ions is expressed as B/A=k, or B = kA. The logarithmic form of this equation is: log B = log A + log k. A plot of A and B on a log-log graph produces a straight line with a 1:1 slope regardless of the value of k; therefore any ion which deviates from this relationship is affected by some process other than that removal of water (Carpenter, 1978).

During evaporative concentration solutes can exhibit three types of behavior (Eugster and Jones, 1979). Type I behavior is characterized by conservative ions which neither precipitates out

during evaporation of the water nor participate in any diagenetic reactions with the subsequent mineralogical environments (Carpenter, 1978). Hence, a plot of a conservative ion concentration versus degree of evaporation would be a straight line. In this case, chloride and bromide are predominantly used as conservative ions when considering the evaporation of seawater. Chloride remains conservative until the precipitation of halite, and bromide is conservative until late stage bittern precipitation (Valyashko, 1956; Zherebtsova and Volkova, 1966).

In evaporative concentration a second type of solute behavior also is exhibited by ions which are directly involved in mineral precipitation. This type of behavior is further subdivided into a Type IIa and IIb (Eugster and Jones, 1979). Group IIa ions are extracted from solution at the onset of mineral precipitation and continue to be depleted by additional mineral precipitation. Once precipitation has stopped, the solute then increases in concentration at a constant rate. Sulfate exhibits this type of behavior during the evaporation of seawater and gypsum precipitation. Group IIb solutes are ions that are removed from solution at the initiation of mineral precipitation and continue to be removed with additional evaporation until they are no longer present in solution. At that point mineral precipitation ceases. During seawater evaporation calcium exhibits this behavior from the onset of gypsum precipitation until gypsum precipitation ceases and no more calcium is present.

The third type of solute behavior during evaporative concentration has been characterized as a Type V solute behavior (Eugster and Jones, 1979). The solute increases in concentration

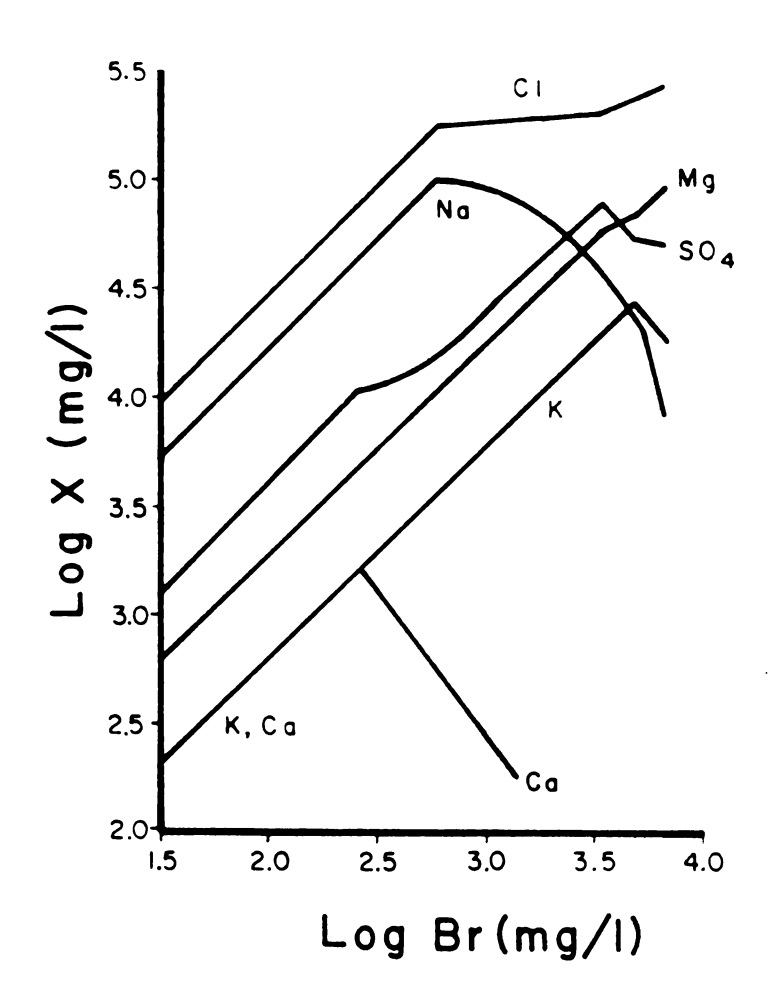


Figure 4. Concentration trends of ions in sea water with evaporation (after Carpenter, 1978)

during the removal of water until it becomes saturated and begins to precipitate. Since this type of behavior is solubility controlled, the concentration of the solute is constant from the point of mineral precipitation regardless of how much additional water is removed from solution. Silica has been observed to display this type of behavior (Eugster and Jones, 1979). For example, in Lake Madadi basin silica never reached a concentration of greater than 60 ppm even though chloride increased by three orders of magnitude.

Carpenter (1978) has developed a computer program to generate a plot of solute behavior during evaporative concentration of seawater. The plot shown in figure 4 represents the chemical evolution of the major solutes in seawater during evaporative concentration. The major points of deflection for the different ions are at the initiation of gypsum, halite, magnesium sulfate and sylvite precipitation.

Solute fractionation - In this geochemical mechanism solute fractionation is a result of processes other than mineral precipitation. Fractionation of ions is a result of: a) selective dissolution of efflorescent crusts, b) selective dissolution of sediment coatings, d) ion sorption on active surfaces, d) degassing of the water, and 3) redox reactions (Eugster and Jones, 1979).

Efflorescent crusts are produced as a result of capillary action drawing interstitial waters upward where it then evaporates and produces a precipitate. Selective dissolution of this crust occurs when surficial runoff seeps down into the sediment. The selective dissolution of the more soluble salts produces a pronounced

fractionation of some ions. This can be demonstrated by the dissolution of a small amount of halite. Since the concentration of sodium in halite is 390,000 ppm, the dissolution of halite and not the remaining precipitates will result in a solution that is strongly fractionated with respect to sodium and chloride.

Dissolution of sedimentary coatings and diagenetic cements can also result in water with a significant fractionation of the solutes. Levy (1977b) proposed that the origin of a calcium chloride brine within the Bardawil sabkha was the result of a brine that was produced by evaporative concentration interacting with calcium carbonate within the sediment.

The sorption of ions on active surfaces can significantly deplete the solution of certain ions. This fractionation of ions is characterized as a Type III or Type IV solute behavior (Eugster and Jones, 1979). Type III behavior is characteristic of solutes that are removed from the water when the removal mechanism or combination of mechanisms is not concentration dependent. Type IV behavior is characteristic of an ion removed only during a limited range of water evaporation. Potassium can exhibit these types of behavior. It can be selectively adsorbed by swelling clays within the sediment (Grim, 1968), and it can be adsorbed by aluminosilicate gels (Jones et al., 1977). Cation anion exchange within clays can also produce a solute fractionation by extracting ions from solution and introducing a substitute ion into the solution.

Redox processes, such as bacterial sulfate reduction can result in solute fractionation. Degassing of solution as a result of variations in temperatures can result in loss of CO<sub>2</sub>. This effect on the

carbonate system can result in solute fractionation by the resultant variations in carbonate solubilities.

Brine mixing - In this process the geochemical composition of the water is a direct result of a mixing of two chemically distinct The mixing of two different brines can result in the precipitation of salts (Raup, 1970) and carbonates (Runnells, 1969; Badiozamani, 1973; Wigley and Plummer, 1976). Conservative properties such as solute concentrations, temperature, alkalinity, acidity and total carbon (Stumm and Morgan, 1970) will display a linear relationship. This linear relationship is a function of the value present in the end member parent solutions and the proportion of each parent in the mixture. The non-conservative properties such as pH, Eh and activities will display a non-linear relationship. relationship means that the mixture can contain a value of the property that is greater or less than that of either parent. The non-linear behavior of these properties has been attributed to three processes; the algebraic effect, the Pco2 effect, and the ionic strength effect (Wigley and Plummer, 1976).

The algebraic effect is produced as a result of the non-linear behavior of the ion activity products during brine mixing. This behavior has been proven experimentally (Wigley and Plummer, 1976). For example, a mixture, with both parents undersaturated with respect to a mineral, can become saturated with respect to that mineral. Raup (1970) produced the precipitation of salts by the mixture of artificial or seawater derived brines. In a mixture of two seawater derived brines a salt precipitated. This salt was predominantly halite with minor amounts of sylvite. In the dorag model

(Badiozamzni, 1973) the non-linear behavior of the ion activity product has been hypothesized as the mechanism for dolomite precipitation. The mixing of meteroic waters with 5 to 30% seawater will produce a solution that is saturated with respect to dolomite and undersaturated with respect to calcite.

In the  $P_{\text{CO}}$  effect, the most important in the carbonate 2 system (Wigley and Plummer, 1976), the mixture of two brines produces a change in the  $\text{CO}_2$  content of the system. This can be produced by the variation in water temperature that is produced by mixing two water bodies at different temperatures. A decrease in  $\text{CO}_2$  of the waters can result in the precipitation of calcium carbonate.

The ionic strength effect is produced by the non-linear dependence of activity coefficients on the ionic strength. In the extreme case, two solutions, both saturated with the same mineral, can become undersaturated with respect to the mineral. This can produce dissolution of the subsequent mineralogical environment.

## **OBSERVATIONS**

## Trends

The waters of the Laguna Madre sabkha are essentially Na-Cl brines that are depleted in Ca, with respect to sea water. Using bromide as a conservative indicator, samples collected in August ranged between 3.5 to 8.9 times the concentration of sea water; likewise, samples collected in March ranged between 3.4 and 9.7 times the concentration of sea water. Chemical analysis of the water samples from the basin, well set B and well site 10, indicate that these waters are distinct from those at sites 9 through 18; because of this the basin region will be discussed separately.

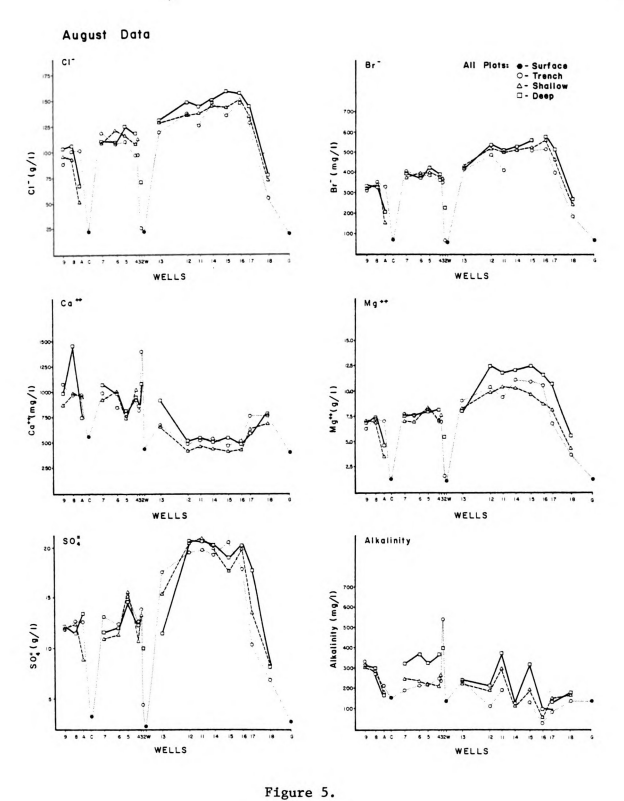
The Intracoastal Waterway and gas well access canals have a negligible effect on all sample sites except site 2. This site is 20 m from the Intracoastal Waterway and appears to be effected by the wake of barges which churn the waters along the shores of the Waterway.

The chloride, potassium, sodium, bromide, magnesium, and sulfate concentrations for well sites 9 through 18 all exhibit similar trends (Figs. 5-8). A concentration plateau exists for these solutes with the maximum values found at well sites 15 and 16. Concentrations decease sharply east of this plateau and gradually west of it. In general, chloride, potassium, sodium and bromide concentrations at each well site increase with depth, while magnesium and sulfate,

sampling (Day 1) to the second day (Day 2) the strontium concentrations increased. Concentrations of calcium ranged from 420 mg/1 to 1080 mg/1 for August with similar values for March. Strontium concentration ranged from 11 mg/1 to 50 mg/1 for August with March values slightly lower.

Alkalinity is mostly in the form of HCO<sub>3</sub> at the pH levels found in these waters. Trench waters had the lowest alkalinity for each well site, with the shallow and deep samples having higher values. Alkalinity was highest for the westernmost well sites and decreased in an easterly direction.

In general, the chemical trends of the major ions within the subsurface waters remained relatively constant between August, 1979 and March, 1980. Salinities increased with depth and the highest concentrations were found approximately 3 km west of the Gulf of Mexico.



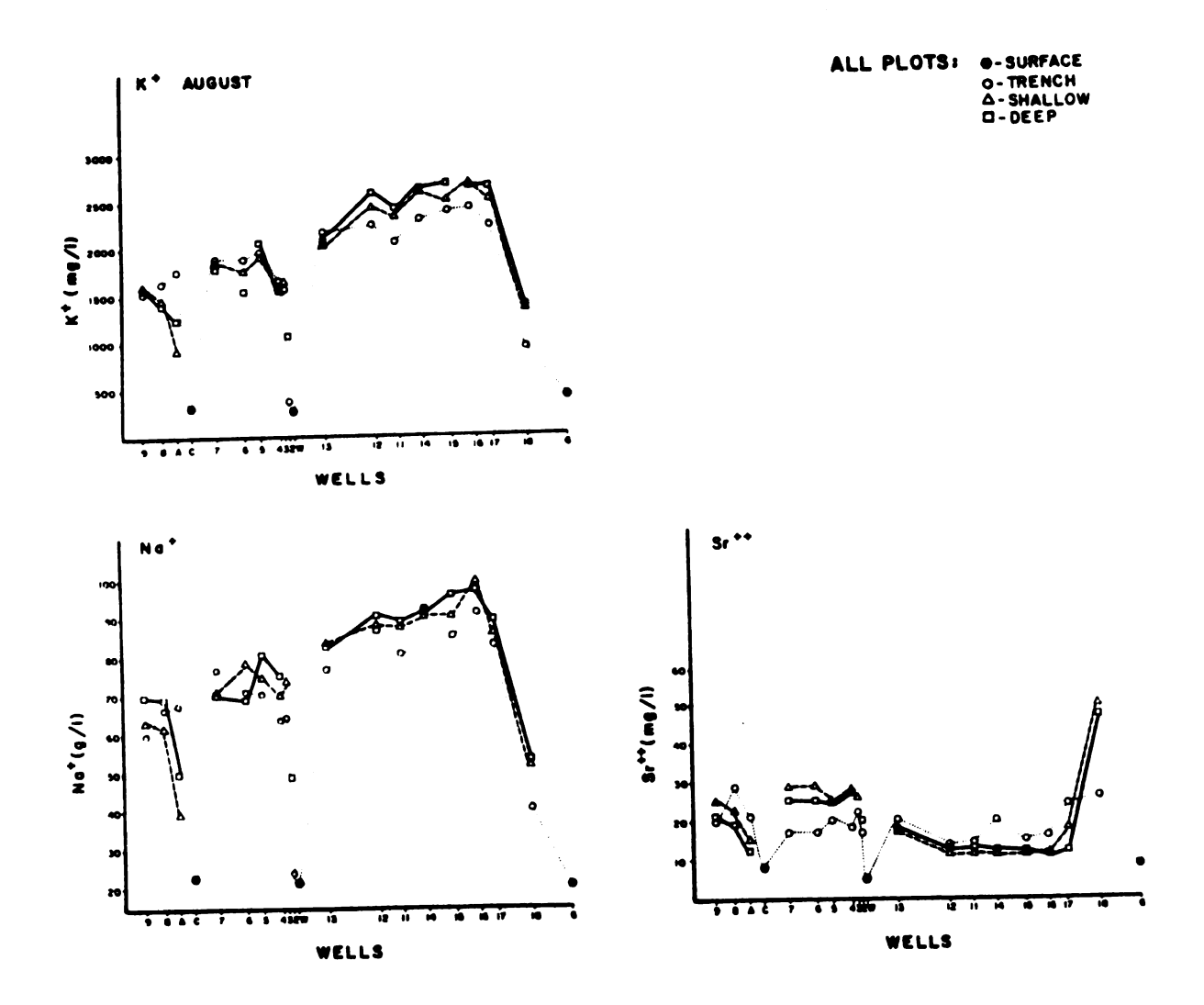


Figure 6.

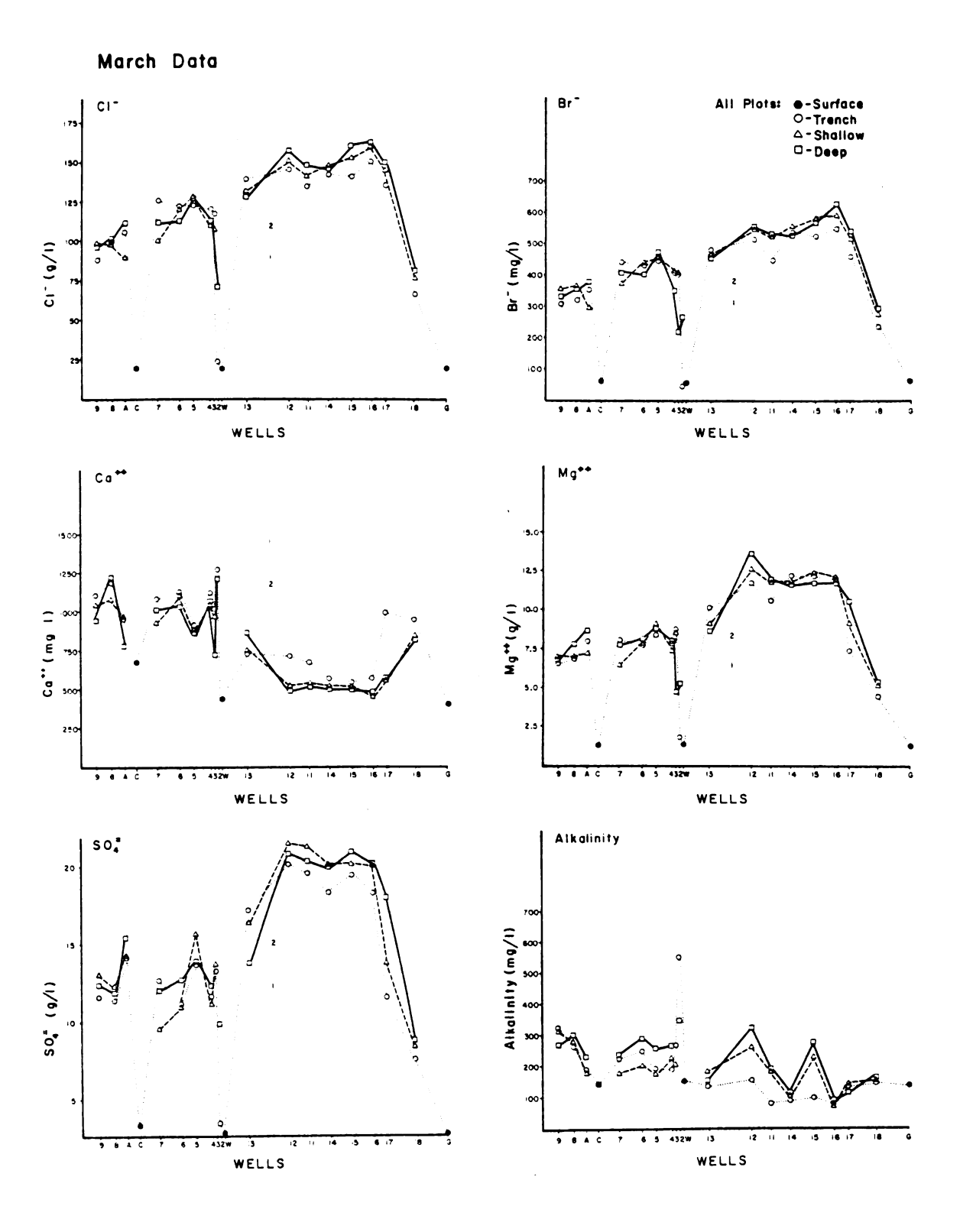


Figure 7.

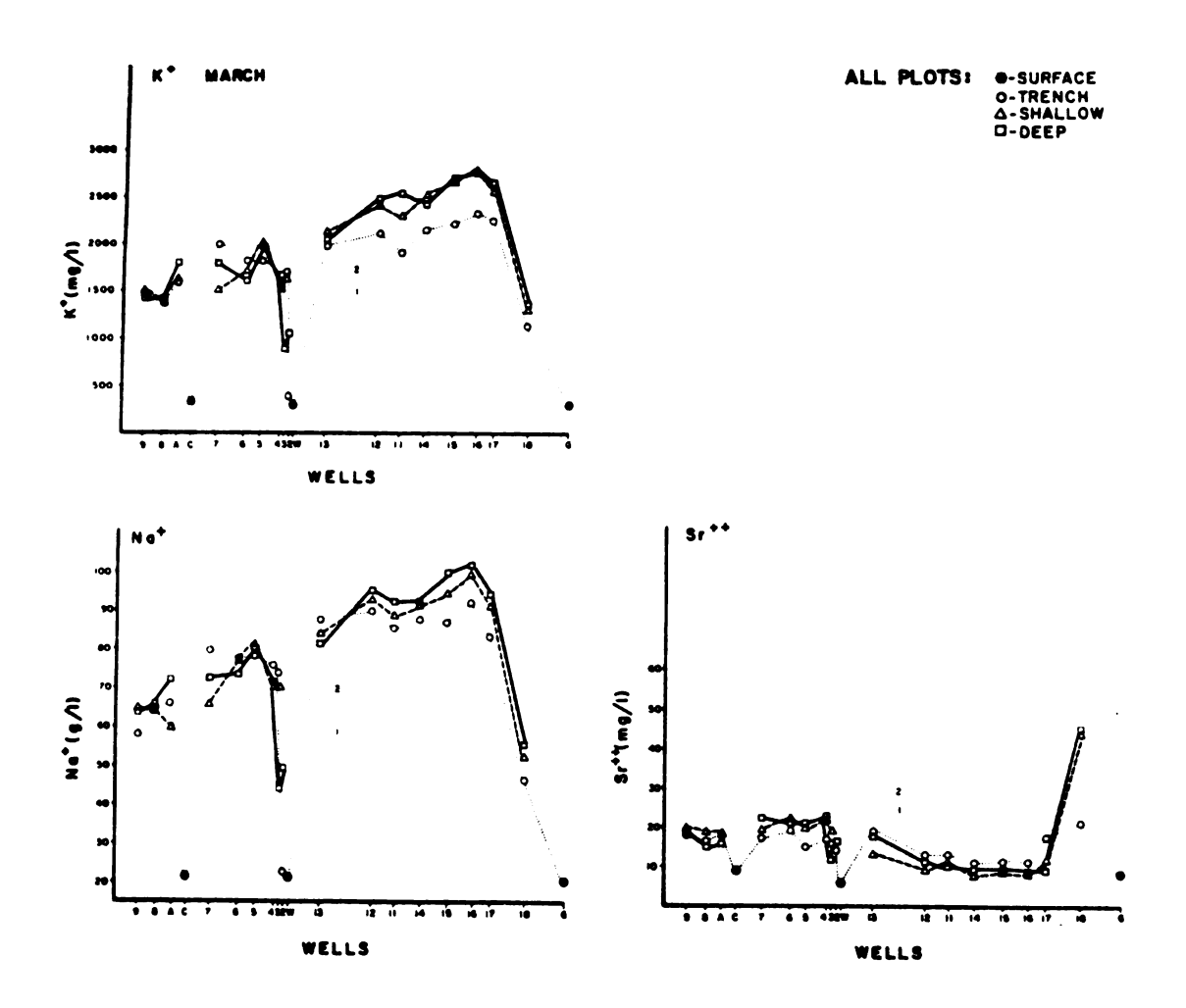


Figure 8.

•
•
•
`
•
•
•
•
•

## PLEASE NOTE:

PAGE NUMBER 46 IS MISSING IN NUMBER ONLY AS TEXT FOLLOWS. FILMED AS RECEIVED.

UNIVERSITY MICROFILMS INTERNATIONAL

## DISCUSSION

There are four possible source regions for the Laguna Madre sabkha brines: sea water from the Gulf of Mexico, water from the Laguna Madre, continental water from the Tertiary Goliad Sand aquifer, or groundwater from the Quaternary eolian plain deposits.

The Goliad Sand is the principle fresh water aquifer for this region. It consists of fine to coarse calcareous sand interbedded with sandstone. It outcrops westward of the study area and dips eastward where it reaches a depth of greater than 300 m beneath the tidal flats. The molar ratios of the conservative ions within the waters of the Goliad Sand aquifer (Table 2) have been calculated from well samples within the area classified as fresh water (less than 1000 mg/1 total dissolved solids) (Shaver and Baker, 1973).

The Quaternary eolian plain deposits are the windblown sediments that completely cover the bedrock surface in the region. It consists of unfossiliferous, massive, fine to very fine sand, and highly calcareous clay. The eolian plain deposits contain a small quantity of slightly saline to very saline waters (1410 mg/1 to 28000 mg/1 chloride concentrations) (Shafer and Baker, 1973).

The molar ratios of the sabkha brines were derived from sample waters taken from well sites along traverse 9 through 18. Well sites A, 17 and 18 were not considered because of their proximity to islands. Well site A is close to a small island while 17 and 18 is

near Padre Island. Chemical trends (Figs. 5-8) indicate a possible influence on these well sites by the fresh water lenses of these islands. In order to more accurately define the average molar ratios of the brines, these well sites were not included in the determination of these values.

In general, the molar ratios (Table 2) indicate that the dominant source region for the sabkha brines is the Laguna Madre. This conclusion is supported by a field observation in March, 1980 of surface flooding in the area produced by winds pushing Laguna Madre waters onto the tidal flats. Although the molar ratios of the Gulf of Mexico and the sabkha brines are similar, the Gulf of Mexico is not the direct parent of the sabkha brines. If this was the case, the chemical trend across the sabkha (Figs. 5-8) would show an increase in concentration with increasing distance from the Gulf. The opposite trend is observed. If fresh water was effecting these trends, then one would expect the molar ratios of the brines to be different from that of sea water. In addition, the Laguna Madre waters more clearly reflect the brine molar ratios.

Variability in Laguna Madre water composition is seen in Figure

9. This variability is attributed to the isolation of the lagoon from
the Gulf of Mexico. River input into Laguna Madre along with
precipitation and high evaporation rates, produce this variability.

This variability is also reflected in the molar ratios of the brines.

Solute behavior within the sabkha brines is characteristic of a parent water body, similar to sea water in composition, but effected by the evaporative concentration process. Bromide, chloride, sodium and magnesium exhibit a Type I solute behavior (Eugster and Jones, 1979) while calcium, strontium, and sulfate exhibit Type II behavior.

-49-MOLAR RATIOS

Source	K/Mg	C1/Mg	Na/Mg	K/C1	Na/Cl	Na/K
Goliad aquifer	0.970	35.4	73.2	0.300	21.290	74.50
Eolian plain	0.057	11.7	11.1	0.005	0.944	194.67
seawater	0.175	9.7	8.2	0.018	0.852	47.00
August ICWW	0.153	16.7	11.1	0.009	0.662	72.44
August canal	0.143	12.6	10.3	0.011	0.816	71.44
March ICWW	0.137	12.6	8.6	0.011	0.685	62.93
March canal	0.145	16.8	8.9	0.009	0.531	61.45
August trench	0.145	11.1	8.2	0.013	0.741	56.47
August shallow	0.151	11.5	8.9	0.013	0.782	58.72
August deep	0.139	10.2	8.1	0.013	0.805	60.39
March trench	0.125	8.5	7.9	0.015	0.949	63.34
March shallow	0.131	9.4	8.0	0.014	0.849	61.09
March deep	0.129	9.0	7.9	0.015	0.885	61.51
August and March 17 & 18	0.166	9.9	9.0	0.017	0.925	54.37
August Well A	0.163	13.1	9.0	0.012	0.689	55.20

A plot of sulfate and calcium versus chloride (the conservative indicator of the degree of water removal)(Fig. 10) indicates that both calcium and sulfate fractionate concurrently. From this is it evident that calcium and sulfate fractionation is a result of the precipitation of gypsum. This geochemical behavior is supported by the field observation of selenite crystals occurring <u>in situ</u> at various well sites.

The molar ratios of the conservative ions are similar to those of sea water; however, those ratios involving potassium show a slight depletion in that ion. This indicates that a minor amount of solute fractionation of potassium occurs within the interstitial brines (Table 2). A possible mechanism for this is cation—exchange with clays. Ililite, which has been reported in the area (Fisk, 1959; Van Andel and Poole, 1960) has a cation—exchange capacity of 10 to 40 meq/100g of clay (Grim, 1968) and therefore could produce this observed fractionation of potassium. Calcium, magnesium and sodium can also be exchanged by illite; however, potassium is the most easily "fixed" ion in illites (Grim, 1968, p. 220). The other ions can be taken up by illites and with changing conditions be released again into the solution. However, this fixation of potassium by illites can permanently remove it from solution and, therefore, account for its slight deficiency.

Unless otherwise noted, data are for Laguna Madre Key to letters used in Figure 9. in the Wind Tidal Flat area. Table 3:

LETTER	LOCATION	SAMPLE DEPTH	SOURCE
   	Flats, 1974	0.1 meters	Lind (1979)
В	Flats, 1972	0.1 meters	Ratzlaff (1976)
S	Flats, 1973	0.1 meters	Ratzlaff (1976)
D	Flats, 1970	1.5 meters	Hahl and Ratzlaff (1975)
ы	Flats, 1969	0.3 meters	Hahl and Ratzlaff (1972)
FI	Flats, 1969	5.3 meters	Hahl and Ratzlaff (1972)
ტ	Gulf, 1969	14.5 meters	Hahl and Ratzlaff (1972)
Н	Flats, 1977	unknown	Amdurer (1978)
J	North of	unknown	Fisk (1959): average*
×	5 Mi. North of Flats, 1949	unknown	Fisk (1959): minimum*
Ľ	lats,	unknown	Fisk (1959): maximum*
X	4 Mi. South of Flats, 1949	unknown	(1929):
Z		unknown	Fisk (1959): minimum*
0	4 Mi. South of Flats, 1949	unknown	Fisk (1959): maximum*
×	Flats, March, 1979	1.0 meter	This Study
Y	Au	1.0 meter	This Study

\* Refers to average, minimum, and maximum concentrations recorded by Fisk (1959) for the samples

area.

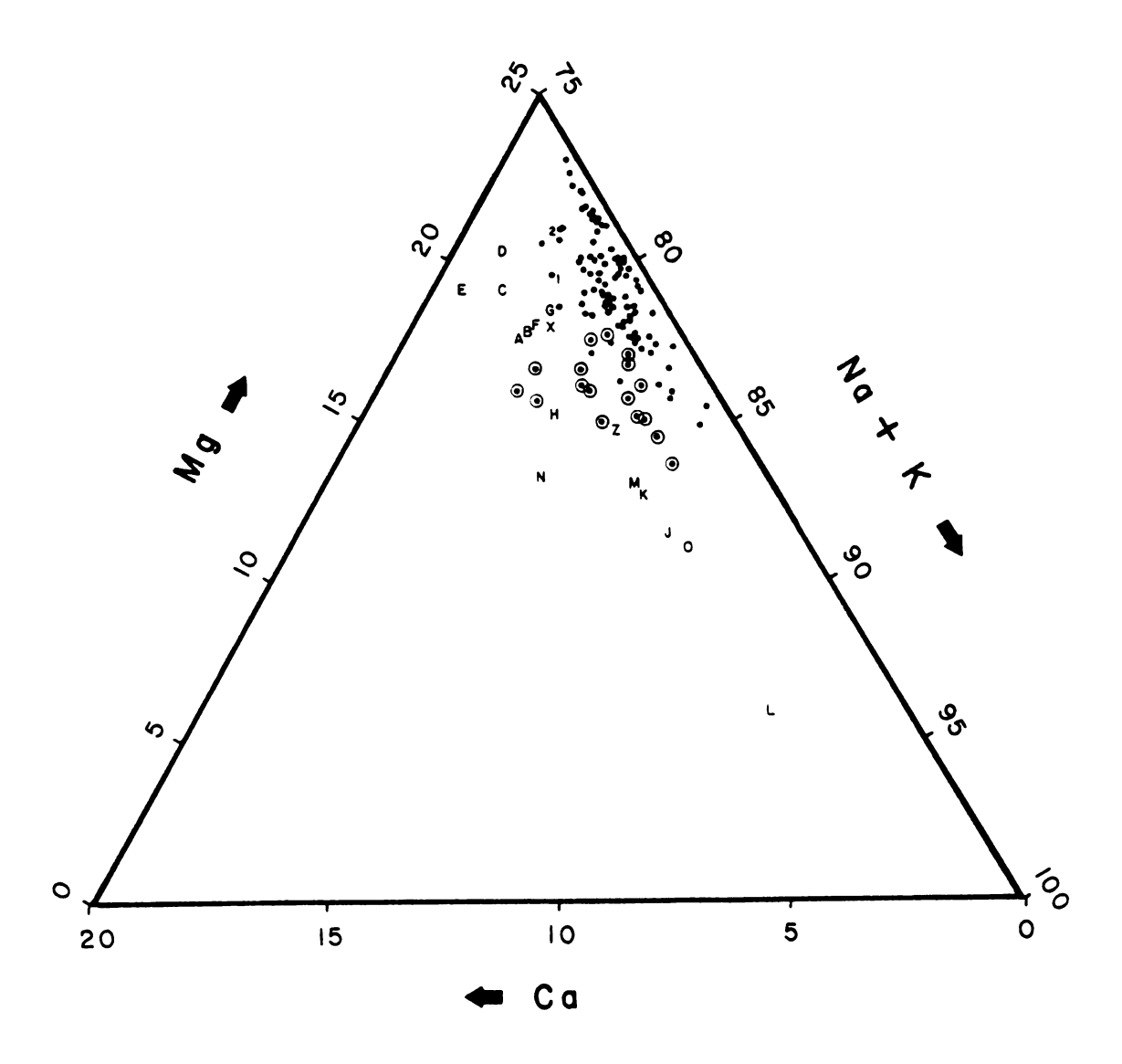


Figure 9. Trilinear plot of samples and Laguna Madre waters.

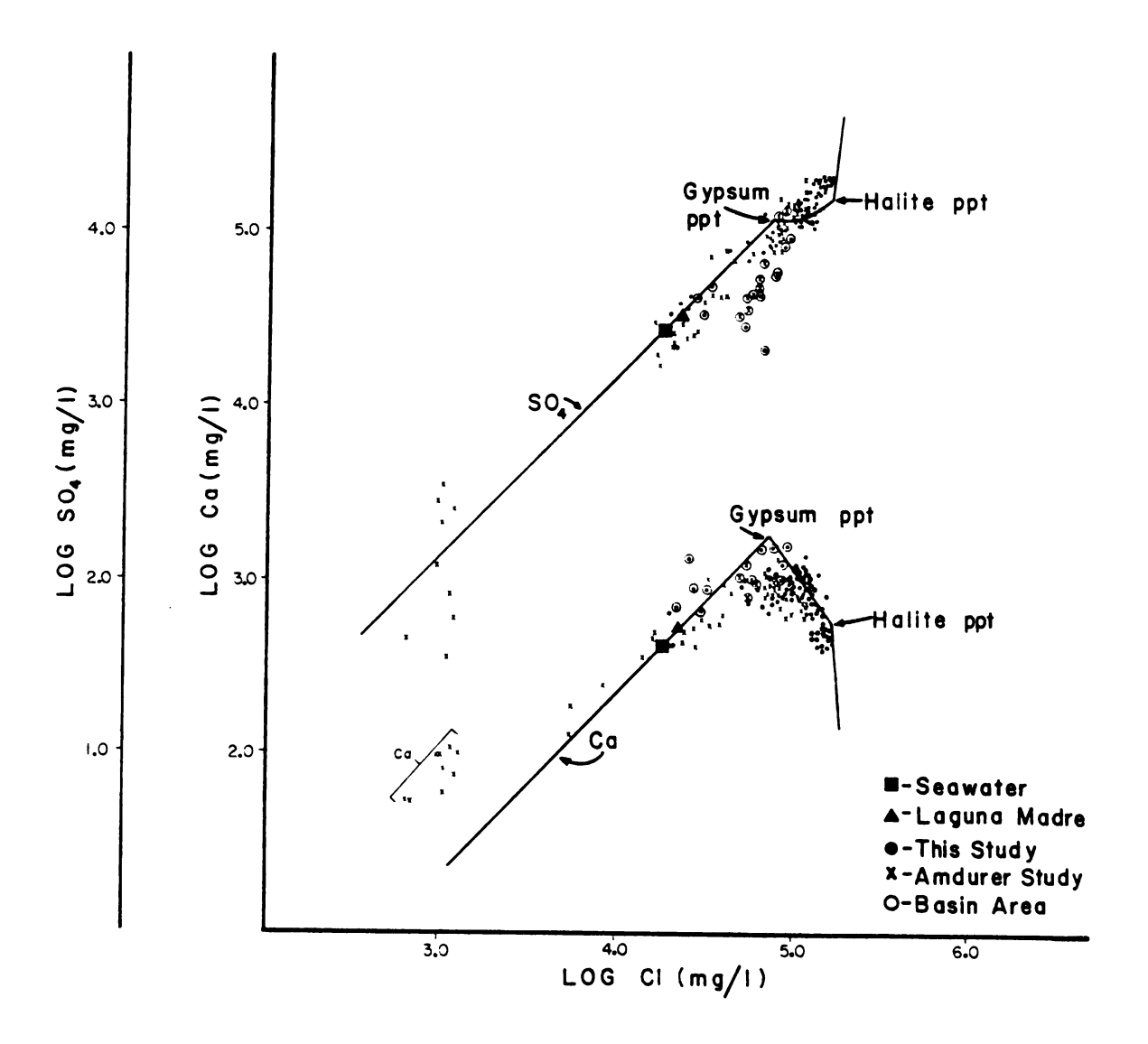


Figure 10. Concentration trends of samples.

#### HYDROLOGY

The hydrology of an active sabkha has long been the subject of debate. Because of their inaccessibility and inhospitable environments, little hydrological data has yet been obtained for an active sabkha. This has resulted in the formulation of the various hydrological models mostly from theoretical considerations, laboratory experimentation, and the presence and zonation of the various evaporitic minerals (including dolomite) within the sabkha. The four major hydrological models that have been proposed are; a) seepage reflux (Adams and Rhodes, 1960), b) capillary action (Friedman and Sanders, 1967), c) evaporitic pumping (Hsu and Siegenthaler, 1967) and d) flood recharge (Butler, 1969). The validity of these hydrological models are based on their ability to generate highly concentrated brines and produce a high enough flow rate through the sabkhas sediments to explain the presence of recent dolomites, and the great thicknesses of ancient supratidal dolomites (Friedman and Sanders, 1967; Hsu and Siegenthaler, 1969). It has only been recently that actual hydrologic field data for an active sabkha has been obtained (Kinsman, 1969; Hsu and Schneider, 1973; Amdurer, 1978). Only Amdurer (1978) has integrated the hydrology of the system with the geochemistry of the brine. However, this study did not accurately define the system because of the limited area of sample sites. One objective of this thesis is to test the hypothesis that evaporitic

pumping is the major hydrologic process operating within the Laguna Madre sabkha. This has been done with hydrologic data obtained from manometers at various locations and depths within the sabkha. This section will first define each of the hydrological models, then present the field data, and from this evaluate the proposed hypotheses.

Seepage Reflx - Reflux action is defined as the seaward escape of a dense brine (King, 1947). In the seepage reflux model the sabkha is sporadically flooded and this water collects into evaporitic lagoons (Adams and Rhodes, 1960; Deffeyes et al, 1965). In these lagooms high evaporation results in an increase in surface water concentration and density. This increase in density causes the surface water to sink to the bottom of the lagoon. There the hypersaline brines, because of their high density, have a hydrodynamic head which results in these waters percolating downward through the sediment. Once within the sediment these hypersaline brines reflux seaward. The hydrodynamic head necessary for the waters to seep into the sediment and the resultant flow rate is governed by the sediment permeability. The generation of the hypersaline brines only occurs on the surface of the evaporiic lagoons and not within the sediment (Adams and Rhodes, 1960). According to this model the water table should be above the piezometric surface with both dipping seaward (Fig. 11). Therefore, net water motion is downward and seaward. If this process were operating within the sabkha one would expect to find the density and salinity of the waters to decrease with depth. A density inversion will occur where the more dense waters overlie less dense waters: however, this density inversion at depth is not necessary for this

hydrologic mechanism to operate.

Capillary Action - This model postulates that the vadose water ascends vertically by capillary action (Friedman and Sanders, 1967). ascending water is concentrated by evaporation and forms a caliche like deposit near the sabkha surface. Because evaporation rate is greater than rainfall, these efflorescent crusts are only periodically dissolved by rainwater. The high evaporation rate could, with solution of the efflorescent crusts, result in an increase in concentration of the interstitial brines. A hydrostatic head is not necessary to drive the waters upward (Hsu and Schneider, 1973); instead this flow is accomplished by capillary action. interstitial water adheres to the sediment within the vadose zone, the near surface waters within this zone evaporate and are replaced by additional water from below (much like a candle wick sucking up wax to replace that burned away). The piezometric surface is equivalent to the water table and the piezometric potential does not vary with depth. A continental source region for the interstitial water and a seaward sloping water table are implied for this model (Hsu and Schneider, 1973).

Evaporative Pumping — In evaporative pumping a vertical hydraulic gradient is induced within the interstitial waters "by an upward decrease in hydrodynamic potential during evaporation" (Hsu and Siegenthaler, 1969, p. 11). The flow rate within the sediment is primarily a function of evaporation with sediment permeability having a negligible affect. According to this model the piezometric surface is higher than the water table (Fig. 11) and the piezometric potential increases with depth (Hsu and Schneider, 1973). This results in a

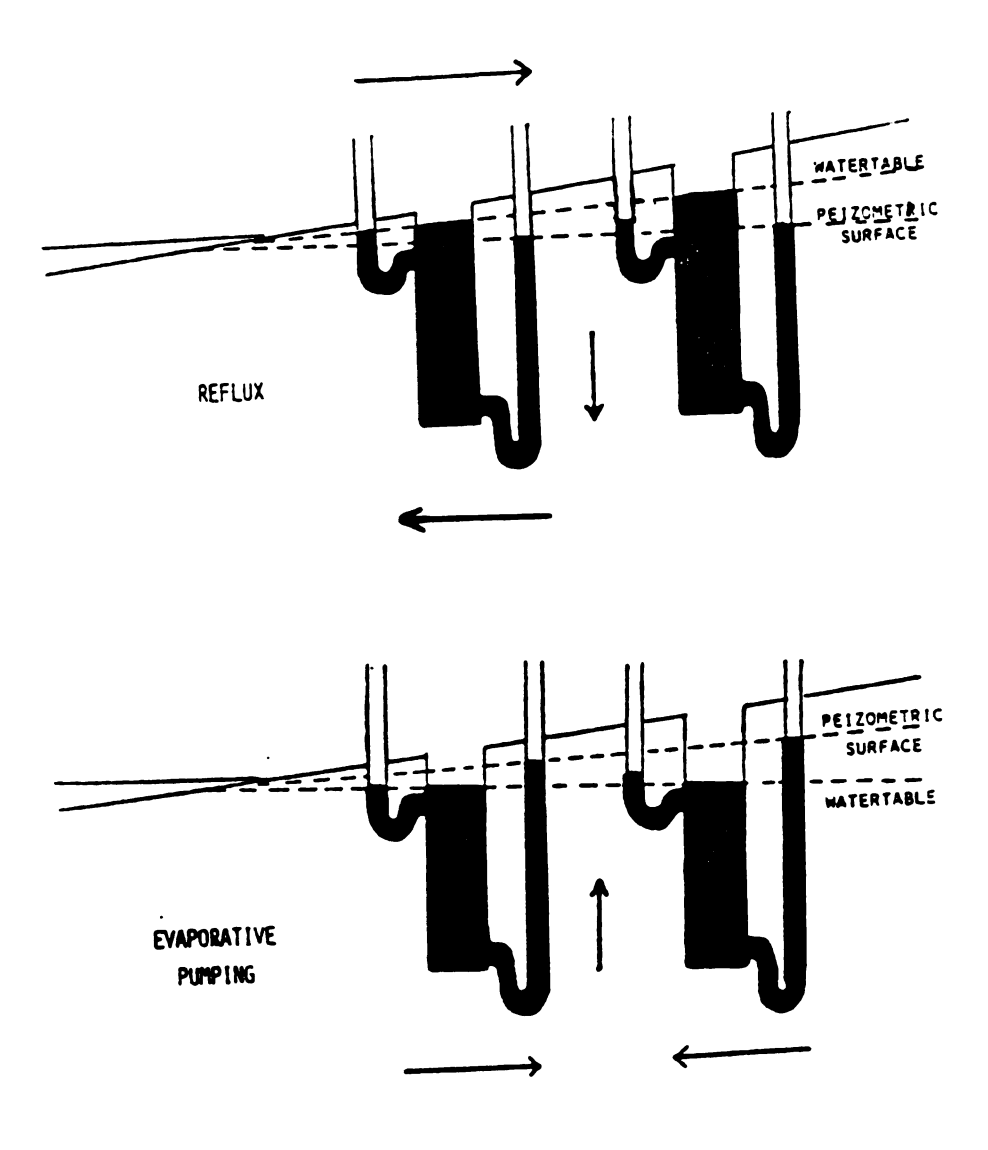


Figure 11. Reflux and evaporative pumping models.

vertically ascending brine (Amdurer, 1978). The source regions for the interstitial waters can be both continental and marine. If the source is continental, then a seaward dipping water table above high tide level should be present. If the water is marine in origin, then the water table, should be equal to or slightly below the high tide level (Hsu and Schneider, 1973).

The development of the Evaporative pumping model was based on laboratory experiments by Hsu and Siegenthaler (1969). It was designed to investigate the potential for this hydrologic mechanism to operate along a highly evaportic coast, to determine what governs the flow rate and, most importantly, to see if this mechanism can generate a flow rate high enough to account for the origin and thickness of recent and ancient dolomites.

In a preliminary hydrologic investigation of the Abu Dhabi sabkha, Persian Gulf, Hsu and Schneider (1973) determined that the piezometric surface was higher than the water table and from this concluded that evaporative pumping was indeed the major hydrologic process operating. However, there were some inherent weaknesses in this preliminary investigation; the major one being some manometers penetrated a zone below an impermeable limestone layer. It was at these sites that the hydrologic head increased with depth. However, this increase could have been produced by a regional head that pushed the trapped waters upward once the impermeable limestone layer was penetrated (Amdurer, 1978). Additional hydrologic data has to be obtained before the hydrologic mechanism operating within the Abu Dhabi sabkha can be determined.

Flood Recharge - Flood recharge occurs when storms and high winds

push sea water onto the sabkha surface and this water then seeps downward into the sediment (Butler, 1969). Flood recharge is not similar to seepage reflux because a density head is not necessary for the waters to descend vertically. The interstitial waters are concentrated by evaporation and solution of soluble salts. According to this model the piezometric potential should not change with depth. A direct correlation should exist between the frequency and extent of flooding, the evaporitic minerals present and the chemical composition of the hypersaline brines (Butler, 1969). The frequency and extent of flooding is related to wind velocity, wind direction, duration and topography. The periodic flooding that occurs with flood recharge rejuvenates the interstitial brines. This hydrologic model allows for local evaporative pumping to occur wherever the frequency and extent of flooding, and the amount of evapotranspiration will determine to what degree it occurs. The recharge water can either be fresh water or marine and movement of the subsurface waters is in direct response to variations in the water table. In the study area, if this were occurring, one would expect the piezometric potential at each well site to be near that of the water table and salinity should gradually increase with depth.

## Observations

A plot of the piezometric potentials as a function of depth for the August and March sampling periods is shown in Figures 12, 13 and 14. The equations used to determine the piezometric potentials and and example are given in Appendix E. During both August and March the piezometric potentials for the majority of the well sites were above that of the Intracoastal Waterway and the Gulf of Mexico In addition, the piezometric potentials for the well sites along traverse 9 through 18 (Fig. 3) show no significant trend with increasing depth. The piezometric surface for well sites 14 through 17 form a plateau with decreasing potential towards the east and west. Since water flows from high to low piezometric potential, it is evident that the interstitial water flow on the west side of the plateau is toward the Intracoastal Waterway, and on the east side towards the gulf.

The hydrologic data for the Laguna Madre sabkha is consistent with a flood recharge model and this is in agreement with the hydrological interpretations for the area by Masson (1955) and Fisk (1959). The data does not support evaporative pumping, seepage reflux or capillary action as the major mechanism operating within the area.

The evaporative pumping model predicts that the area with the highest brine concentration (at the salinity plateau) would have the lowest piezometric potential because water movement should be toward these sites of highest evaporation. Instead, these sites have the highest potentials with water movement away from them. In addition, if evaporative pumping of marine water were occurring, as the geochemistry suggests, the piezometric potential for all the well

sites should be lower than than that of sea water. Instead, the majority of well sites have higher potential (Figs. 12 and 13). Evaporative pumping can operate to a minor degree at some well sites, but it is not the major process controlling interstitial water flow in the area.

A seepage reflux process with a marine source region would require that the piezometric surface dip toward the Gulf. Also, a definite decrease in piezometric potential with increasing depth at all the well sites should occur. Figures 12 and 13 show that although the piezometric potential at most well sites are greater than that of the Gulf, the interstitial waters are not refluxing into the Gulf or into the Intracoastal Waterway. In addition, there is not clear decrease in piezometric potential with increasing depth at the well sites. Therefore, seepage reflux is not the major hyrologic process controlling interstitial water flow in the area.

In capillary action a continental source region with a seaward dipping piezometric surface is required (Kinsman, 1969). The plots of the piezometric potentials for the various well sites indicate that major water flow is not from the continent. In addition, the geochemistry of the waters indicate that these brines are not continentally derived. Both of these observations strongly suggest that capillary action is not the major hydrologic process governing water flow within the study area. However, it is possible that capillary action is occurring to a limited extent near the surface of the study area.

The interstitial waters of the Laguna Madre sabkha appear to respond to a hydrodynamic process in which interstitial water is

recharged by periodic flooding with floodwater seeping into the sediment. Major interstitial water movement is in direct response to fluctuations in water table. This interpretation is consistent with the geochemical predictions about the system discussed in the previous section.

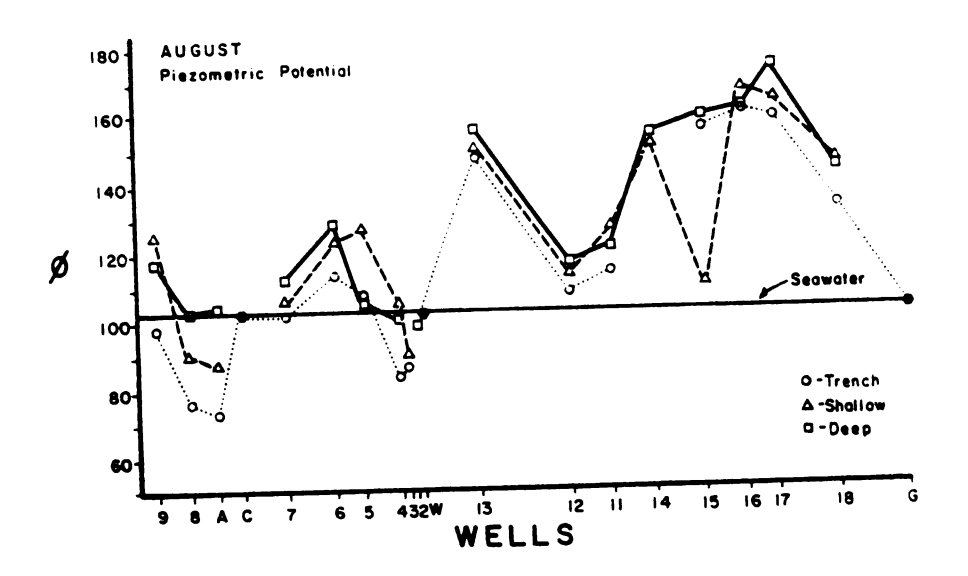


Figure 12.

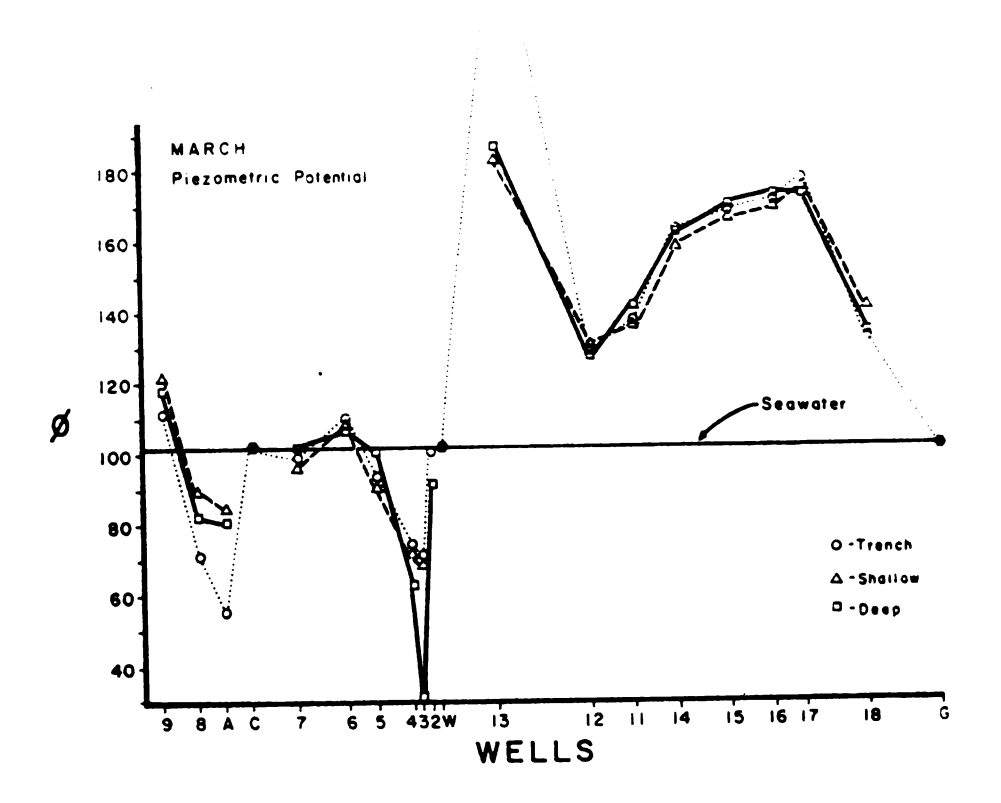


Figure 13.

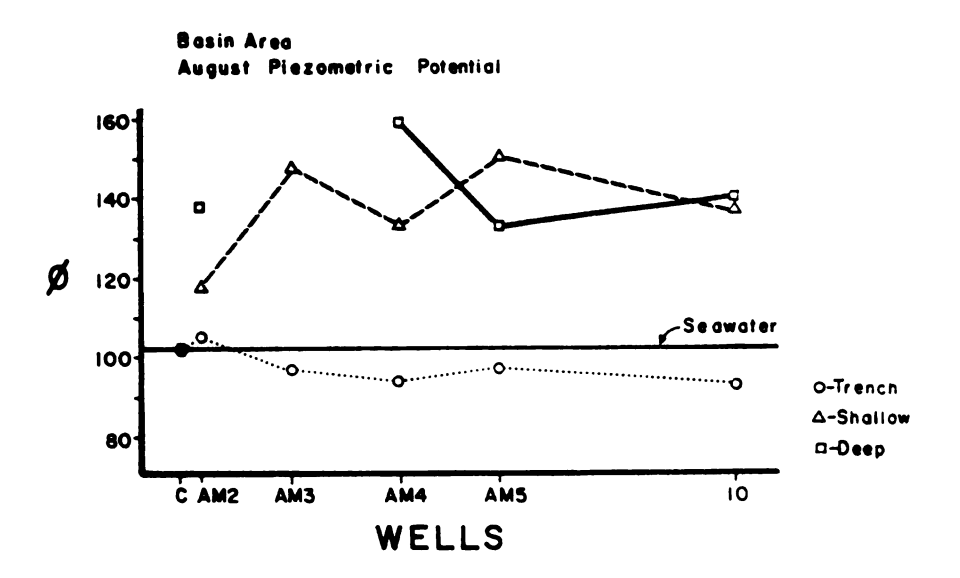


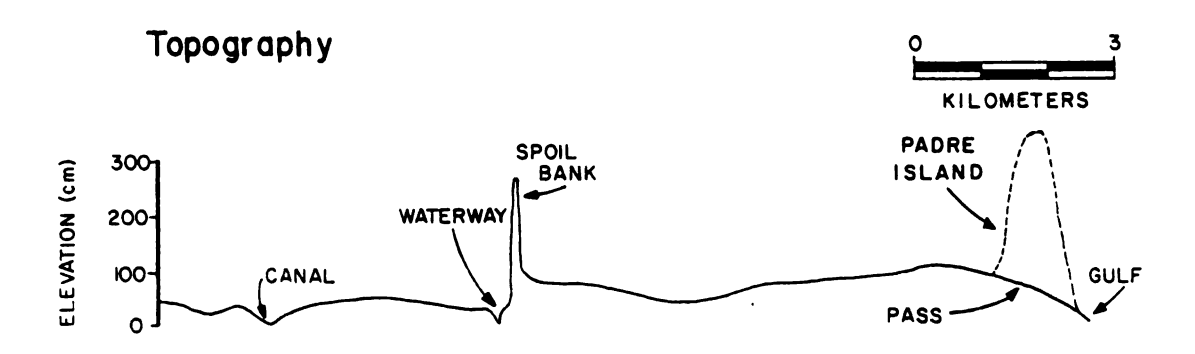
Figure 14.

## Discussion

The piezometric potentials shown in Figures 12 and 13 support flood recharge as the major hydrological process for the Laguna Madre sabkha. Bromide concentration is directly related to the degree of brine concentration because of its conservative nature. bromide contour maps as a funcion of depth can be informative as to the hydrologic nature of the interstitial waters and can be used to relate the geochemisty of the system to the hydrology. The bromide contour maps for the August and March sampling periods (Fig. 15) indicate that there is an increase in bromide concentration with depth, but that the increase with depth is not continuous across the This salinity change with depth is consistent with the flood recharge model. Figure 15 shows that the recharge waters move down as salt fingers rather than as a continuous salt sheet. This pattern of flood recharge was also observed by Butler (1969) for the Abu Dhabi sabkha with the use of chloride contour maps. The bromide contour maps (Fig. 15) also indicate that although actual bromide concentration does vary for the August and March sampling periods the pattern of recharge is similar.

A rapid decrease in bromide concentration at well sites 17 and 18 and for the shallow and deep waters at well site A is seen in figure 14. A greater amount of flood recharge to these well sites cannot account for this decrease in bromide concentration because the molar ratios of the conservative ions within the waters of these sites are slightly different from those of the other sites (Table 2). In addition, the dilution effect at these sites is less for the drier

month of March. This data indicates that the decrease in bromide concentrations for waters at well sites 17 and 18 is due to a dilution effect by the fresh water lens of Padre Island, and that the decrease in the shallow and deep waters at well site A is due to the effect of a fresh water lens from a nearby island (Fig. 3). The decrease in brine concentration along the western side can be caused by two The first is that this area is being recharged in part by continental groundwater (Amdurer, 1978). The bromide contour maps (Fig. 15) do not indicate dilution from below or westward. Therefore the mixing zone between the sabkha's marine groundwater and continental waters most likely occurs westward of well site 9 or at a depth below 3.8 m. The second reason for the dilution effect on these western sites is that they are being rejuvenated more often. Since flood recharge is the major hydrological mechanism in the area, one would expect that the areas that flooded most often would have interstitial waters with comparatively lower concentrations. The well located on the western side of Laguna Madre are at a lower elevation and also near the Intracoastal Waterway and gas well access canals (Fig. 3). Since these well sites have a higher potential for flooding than those on the eastern side, one would expect that their water concentrations would have lower values, this appears to be the situation.



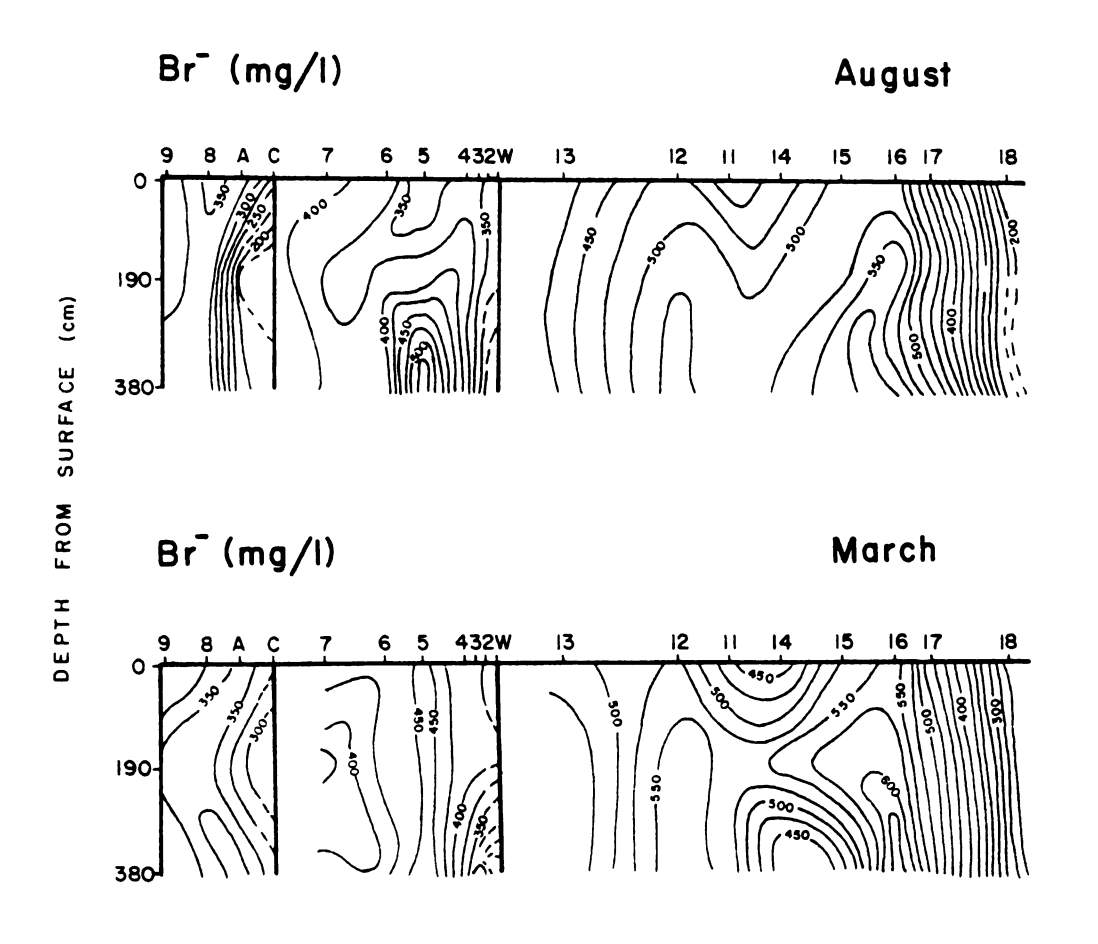


Figure 15. Bromide contour maps.

## Basin Area

The brines within the basin area, well site 10 and well set B, are chemically distinct from those found at the other well sites. Going from east to west, well set B (Fig. 3) includes AM2, AM3, AM4, and AM5. The wells within the basin are characteristically lower in sulfate content and, when considering cation percentages, the basin brines are higher in Ca and lower in Mg (Fig 8). In addition to this area containing distinct waters from those found in the other areas, the chemical trends and molar ratios of the well waters indicate that there are two distinct vertically stratified water masses within the basin. In comparison, the more shallow water is characteristically higher in concentration and has a greater Mg/Ca and lower Cl/Br molar ratio (Table 4).

The ionic ratios of this upper water mass and the waters of the gas well access canal are similar; Table 4 demonstrates that they both have similar Cl/Br ratios and indicates that the Laguna Madre water is the most likely parent for this upper water mass. The higher Cl/Br molar ratio of the deeper water mass cannot be explained by simple evaporative concentration of Laguna Madre water since the ratio between these conservative ions would not be affected by just the removal of water. Therefore, this deeper water mass is either a Laguna Madre water that has been extensively modified by solute fractionation or has a different source region, or is a mixture of Laguna Madre waters and groundwater of continental origin. A Pleistocene river valley underlies the basin area (Fisk, 1959). Since coarser sediment fills this valley continental water could be

Selected chemistries for the basin brines as a function of distance from gas well access Table 4:

			WELL SITES	ITES			GAS WELL SEAWATER** ACCESS CHANNEL	EAWATER**
		10		We11	Well Set B			
	Meters from Channel	852	487	331	175	34		
Br	trench	309	262	317	196	295	68.9	65
mg/1	shallow	305	239	212	NA*	71		
ı	deeb	305	28	174	<del>7</del> 9	54		
C1/Br	trench	099	684	726	722	889	761	629
Molar	shallow	929	736	726	NA*	1064		
	deeb	649	1200	822	983	286		
Mg/Ca	trench	8.1	<b>6.</b> 8	9.7	<b>9.</b> 0	9.7	3.8	5.1
Molar	shallow	6.1	4.5	3.9	NA*	3.7		
	deeb	<b>6.</b> 8	4.1	5.1	3.0	3.1		
	,							

\*NA - no sample

<sup>\*\*</sup> from Goldberg (1963)

channeled to this area by this path. Solute fractionation of Laguna Madre waters would have to be extreme and atypical. This is because all of the major molar ratios of these deeper waters are distinct from sea water. Therefore, solute fractionation would have to affect Br, Cl, and Mg. It would be rare for this major solute fractionation to occur and rarer for it only to occur within the shallow and deep regions of the basin. Since this is not probable, the Laguna Madre is not likely to be sole parent water for this area. The higher Cl/Br molar ratio of the lower water mass indicates a fresher water source (continental)(Patterson and Kinsman, 1977). However, the molar ratios observed are not similar to either of the identified continental groundwater systems (Table 2). Therefore, there is either another continental groundwater system, or more likely this lower water mass is a mixture of the Laguna Madre waters with groundwater continental in origin. Figure 14 is a plot of the piezometric potentials of these wells within the basin. It is evident from this plot that the deeper waters are flowing upward. This direction of flow is the result of either evaporative pumping of the water, or input in the area from a continental source which is under a regional hydrological head (Amdurer, 1978). Amdurer (1978) observed a clay layer within the basin area that separates the trench waters from the deeper waters. The layer could act as a semiconfining stratum and therefore, the artesian condition observed could be the result of the penetration of this layer by the wells. Amdurer (1978) also suggests that the source of these deeper waters is continental in origin. In August, 1980 a field expedition west of well site 10 revealed numerous brackish water springs. The presence of these springs strongly supports the presence

of a regional hydrodynamic head.

The geochemical and hydrological data indicate that the basin is unique in comparison to the rest of the sabkha. In this area two distinct water masses exist. The upper mass most likely has Laguna Madre water as a parent, while the deeper water mass is likely continentally derived. The lower water mass observed within the basin can either be derived from a continental aquifer other than the ones listed in Table 2, or it can be a mixture between the Laguna Madre waters and either continental water from the Golian Sand or Eolian plain aquifers. If the later condition were true, then the clay layer or layers within the basin would act as a semiconfining stratum (Davies and DeWeist, 1966, p. 43), where leakage between the two water masses could occur. This is implied in the upper water mass where the composition is slightly different from typical sabkha brines, as seen on the trilinear graph (Fig. 8).

# Computer Modelling

An additinal technique in describing the chemisty of the interstitial waters and its possible diagenetic interactions with the surrounding sediments is by chemically modeling the water. In order to do this the concentrations, activities, distribution of chemical species in solution and, saturation state of evaporitic minerals must be determined. A modified version of the WATEQ computer program (Truesdell and Jones, 1973) was used in the computer modeling of the Laguna Madre waters. In general this program first determines the analytical cation-anion balance of the solution. This is a first estimate in determining the accuracy of the water analysis. If the solution has a reasonable charge balance, a precursor to further computations, the program then calculates the various chemical and thermodynamic parameters of the solutions. The technique used to determine these parameters is based on the Garrels and Thompson (1962) treatment of sea water where the activities of the unassociated and complexed ions in solution are determined. The program then computes the ion activity products and the solubility products of the various possible minerals that can exist in equilibrium with the solution in order to determine their relative saturation.

The basic concepts and equations that the WATEQ computer program performs and the limitations are as follows. The relative stability of minerals is the Law of Mass Action. This law states that the driving force of a chemical reaction to the right or left is related to the concentrations of the reactants and products. For a system at equilibrium the product of the activities of the reaction products

divided by the product of the activities of the reactants is constant at a given temperature. This constant is the thermodynamic equilibrium constant. This relationship is expressed in the following equation:

$$[MX] = [M^+][X^-]$$
 (1)

where the brackets represent the activities of the chemical species.

This reaction can also be characterized by the equilibrium constant.

$$\frac{[M^+][X^-]}{[MX]} = K \tag{2}$$

Because a mineral is in its standard state its activity is by definition one (Garrels and Christ, 1965, p. 43). Therefore, equation (2) can be rewritten as:

$$Ksp = [M^{+}[X^{-}]]$$
 (3)

Solubility products of major minerals at 25°C have been determined experimentally and are utilized by the program. Variations in temperature affect solubility products; therefore, they are determined for field temperatures.

From the brine composition the ion activity products are determined. This is necessary for considering the saturation state of various mineral. In the determination of the ion activity products the activities of the various ions in solution must be calcualted. Activity of an ion in solution is related to its concentration by the following equation:

$$a_{i} = \chi_{i}^{m_{i}} \tag{4}$$

where  $a_1$  is the activity of the ion,  $m_1$  is the molality of the ion and  $y_1$  is the practical activity coefficient. The activity coefficient is calculated by the use of either the extended

Debye-Huckel or Helgeson equation. The extended Debye-Huckel is used when the ionic strength of the solution is less than 0.1, for monovalent ions, and 0.05 for divalent ins. The extended Debye-Huckel equation is:

$$\log Y_{i} = \frac{-Az_{i}^{2}I^{1/2}}{1+B a'I^{1/2}}$$
 (5)

where A and B are constants, characteristic of the solvent (water), and are a function of temperature;  $z_i$  is the ionic charge of the species considered; I is the ionic strength of the brine (I = 1/2  $m_i z_i^2$ ) and; a' is the hydrated size of the ion (Garrels and Christ, 1965, p. 62-63).

The Helgeson equation can be used at higher ionic strengths in determining the activity coefficient of the minor constituents (less than 10%) in a NaCl solution. This equation is;

$$\log \mathbf{\hat{Y}}_{1} = -Az_{1}^{2}I^{1/2} + B'I \qquad (6)$$

$$1 + B a' I^{1/2}$$

where the first part of this equation is the extended Debye-Huckel and in the second half, B' is the deviation function describing the departure of the mean ionic activity coefficient of an electrolyte from that predicted by the Debye-Huckel equation. This value has been measured for NaCl (greater than 80%) solutions at different temperatures (Helgeson, 1969). The Helgeson method is an addition to the Truesdell and Jones (1969) computer program.

Another consideration in chemical modeling is the determination if ion distribution in solution. When considering the activity of free sulfate in solution the following relationship occurs:

$$mSO_4^{-1}$$
 Total =  $m_{NaSO_4^{-1}} + m_{KSO_4^{-1}} + m_{CaSO_4^{-1}} + m_{MgSO_4^{-1}} + m_{SO_4^{-1}} + m_{SO_4^{-1}}$  free. (7)

The distribution of carbonate species can be determined from alkalinity and pH. This relationship and the known equilibrium dissociations of the various species in equation (7) permits the program to simultaneously solved for all the unknowns and therefore, determine the distribution of the species. One major weakness in this technique is that the program does not consider C1<sup>-</sup> complexes, and only considers first order complexes involving the other species.

The method by which the WATEQ program performs these calculations is by a series of iterations. The determinant factor in these iterations is the ionic strength of the solution. During the first iteration all activity coefficients are set to unity. The program then computes the carbonate distribution from alkalinity and pH measurements. The ionic strength of the solution is then computed and, from this, activity coefficients and species distributions are determined. The program then computes a new ionic strength. This iterative process repeats until the computed new ionic strength equals the previously calculated ionic strength. Once this condition is met, then mineral equilibria, selected ionic ratios and a computed cation—anion balance considering complexing are determined. With this information, geochemical interpretations about the brines and their potential for diagenetic interactions with surrounding sediment can be performed.

Table 7 is the compilation of the computed mineral saturation states of all the water samples analysed in this study. A saturation index of 1 means that the water is in equilibrium with that mineral.

An index greater than 1 means the water is supersaturated, and an

index of less than 1 mean the water is undersaturated with respect to that mineral Most brines, including those of the basin area are supersaturated with respect to dolomite. In addition, dolomite saturation generally increases with depth. Calcite and gypsum saturation vary across the sabkha. In general, for the brines along traverse 9 through 18, there is a tendency for the more concentrated brines to be undersaturated with respect to calcite and gypsum. In August, 1979, the brines along the western side of the sabkha are saturated with respect to dolomite gypsum and calcite, while those along the eastern side are only saturated with respect to dolomite. In March, 1980, this was also true except that the brines along he eastern side were near saturation with respect to gypsum. These eastern brines, therefore, have a high potential for dolomite formation according to the mixing model of Badiozamani (1973). high amount of Sr in well waters of sites 17 and 18 (Fig. 7) might be an indication of aragonite converting to dolomite (Kinsman, 1969).

-78-Table 5

	Sa	turation St	ates (IAP	/Ksp)	August	
Well	Anh yd ri te	Aragonite	Calcite	Dolomite	Gypsum	Ionic Strength
SW	0.228	3.137	5.708	228.8	0.356	0.679
9T	1.124	0.466	0.844	12.16	1.384	3.048
9S	0.922	1.148	2.088	107.9	1.043	3.315
<b>9</b> D	1.089	0.645	1.177	30.64	1.180	3.619
8T	1.080	1.408	2.563	152.2	1.207	<b>3.</b> 505
8S	1.088	0.753	1.371	39.88	1.241	3.219
8D	1.531	0.787	1.435	33.00	1.654	3.695
AM1T	1.169	0.839	1.528	52.71	1.300	3.554
AM1S	0.922	0.730	1.325	17.10	1.178	1.777
AM1D	0 <b>.9</b> 05	0.369	0.670	7.691	1.113	2.364
7T	1.069	0.228	0.418	3.854	1.437	4.084
7S	0.922	1.141	2.081	10.74	0.990	3.749
7D	1.118	0.545	0.993	22.66	1.199	3.796
6 <b>T</b>	0.935	0.159	0.289	2.144	1.051	3.695
6S	1.074	0.704	1.285	37.52	1.120	4.114
6D	1.047	0.351	0.641	10.64	1.131	3.723
5T	1.059	0.204	0.371	4.433	1.161	3.799
5S	1.018	0.340	0.621	14.26	1.074	4.035
5D	1.048	0.282	0.513	8.977	1.103	4.341
4 <b>T</b>	1.024	0.253	0.461	4.913	1.161	3.307
4S	0.996	0.588	1.073	25.55	1.074	<b>3.7</b> 00
4D	1.052	0.374	0.680	1.298	1.129	4.091
3T	0.985	0.171	0.311	2.521	1.116	3.310
<b>3</b> S	1.032	0.360	0.656	12.14	1.118	3.928
2T	0.830	2.721	4.996	61.52	1.377	0.854
2D	1.033	0.651	1.188	20.66	1.212	2.458
13T	1.004	0.363	0.661	19.38	1.050	4.161
13S	0.938	0.501	0.914	0.525	35.67	4.496
13D	0.984	0.250	0.455	6.245	1.023	4.509
12T	0.845	0.052	0.094	0.654	0.842	4.859
12S	0.761	0.198	0.362	10.66	0.744	4.796
1 2E	0.956	0.203	0.371	11.89	0.926	5.329

-79Table 5 (continued)

		Saturation	States (	IAP/Ksp)	Augu	st
Well	Anhyd rite	Aragonite	Calcite	Dolomite	Gypsum	Ionic Strength
11T	0.920	0.131	0.239	3.406	0.926	4.404
11S	0.863	0.380	0.695	36.92	0.842	<b>3.</b> 852
11D	0.990	0.387	0.704	37.35	0.992	5.134
14T	0.989				0.971	5.375
14S	0.794	0.097	0.178	2.620	0.761	5.067
14D	0.933	0.086	0.158	2.148	0.880	5.361
15T	0.828	0.135	0.247	4.834	0.840	4.795
15S	0.634	0.133	0.243	4.820	0.613	4.938
15D	0.975	0.252	0.461	18.04	<b>0.9</b> 00	5.663
16T	0.840	0.074	0.135	1.323	0.828	5.166
16S	0.808	0.052	0.095	0.651	0.789	5.299
16D	0.914	0.061	0.112	1.087	0.849	5.547
17T	0.749	0.230	0.418	5.148	0.819	4.357
17S	0.798	0.203	0.369	5.870	0.839	4.633
17D	0.949	0.144	0.261	4.257	0.974	5.072
18T	0.578	0.584	1.061	14.44	0.736	1.834
18S	0.570	0.512	0.929	15.21	0.711	2.446
18D	0.613	0.667	1.210	27.20	0.758	2.623
CAM2	0.361	5.770	1.056	640.4	0.460	0.752
ICWW	0.226	3.468	6.347	247.6	0.289	0.674
10T	1.045	1.313	2.383	80.85	1.274	2.830
10S	1.282	0.514	0.936	9.902	1.473	3.073
10D	1.009	0.491	0.895	9.946	1.141	2.959
am 5t	0.654	0.691	1.256	18.93	0.789	2.642
AM 5S	0.379	1.265	2.299	32.62	0.507	1.028
AM 5D	<b>0.9</b> 20	0.714	1.297	13.31	1.114	2.604
AM4T	1.061	0.624	1.135	23.61	1.197	<b>3.</b> 500
AM4S	0.341	0.775	1.407	16.43	0.437	1.720
AM4D	0.359	1.875	3.405	77.62	0.446	2.222
AM 3T	0.419	1.332	2.420	59.39	0.524	2.062
AM3S	0.621	1.995	3.625	58.95	0.834	0.967
AM 2T	0 <b>. 97</b> 0	0.674	1.225	26.40	1.139	3.080

-80Table 5 (continued)

	Sa	turation St	March			
Well	Anhyd rite	Aragonite	Calcite	Dolomite	Gypsum	Ionic Strength
AM2S	0.459	0.273	0.469	1.137	0.623	0.814
AM 2D	0.668	2.812	5.109	147.5	0.888	1.149

-81Table 5 (continued)

	Saturation States		ates (IAP	(IAP/Ksp) March		
Well	Anhyd rite	Aragonite	Calcite	Dolomite	Gypsum	Ionic Strength
9T	1.029	0.161	0.297	1.356	1.530	3.003
<b>9</b> S	1.111	0.361	0.660	8.076	1.532	3.403
<b>9</b> D	0.973	0.160	0.692	1.705	1.346	3.345
<b>T</b> 8	1.115	0.231	0.427	2.780	1.610	3.410
8S	1.085	1.964	3.593	228.0	1.502	3.350
8D	1.170	1.303	2.383	103.2	1.603	3.539
AM1T		0.183	0.334	2.718		3.601
AM1S	1.109	0.315	0.576	6.736	1.559	3.149
AM1D	0.976	0.120	0.219	1.545	1.300	3.935
7T	1.144	0.123	0.227	1.115	1.532	4.318
7S	0.754	0.573	1.048	21.46	1.037	3.409
7D	1.009	1.198	2.190	107.2	1.341	3.880
6T	1.050	0.142	0.263	1.344	1.438	4.158
6S	1.048	0.310	0.565	6.722	1.342	4.154
6D	1.111	0.362	0.660	9.997	1.441	3.969
5T	1.038	0.155	0.285	2.190	1.380	4.276
5S	1.167	0.305	0.556	9.984	1.457	4.510
5D	1.006	0.159	0.291	2.641	1.278	4.419
4T	1.638	0.081	0.148	0.507	1.932	5.834
48	0.976	0.205	0.375	2.864	1.315	3.745
4D	1.091	0.235	0.429	3.954	1.460	3.855
<b>3</b> T	1.071	0.063	0.116	0.331	1.481	4.082
3S	1.071	0.162	0.296	2.073	1.442	3.769
3D						2.093
2T	0.664	2.297	4.247	5.401	1.141	0.862
2D	1.052	0.296	0.541	3.276	1.544	2.471
13T	1.052	0.740	0.135	0.815	1.277	4.920
138	1.023	0.428	0.783	22.61	1.298	4.605
13D	0.983	0.083	0.152	0.700	1.276	4.432
Dayl	1.580				1.926	3.065
Day2	1.510	2.210	4.008	36.98	1.749	3.846
12T	1.156	0.204	0.377	7.107	1.502	5.181

-82Table 5 (continued)

		Saturation	States (I	AP/Ksp)	Ma <b>r</b> ch	
Well	Anhydrite	Aragonite	Calcite	Dolomite	Gypsum	Ionic Strength
1 2S	0.909	0.427	0.788	46.81	1.147	5.429
12D	0.855	0.190	0.350	10.86	1.060	5.716
11T	1.065	0.045	0.083	0.326	1.383	4.827
118	0.902	0.144	0.264	4.780	1.139	5.076
11D	0.860	0.113	0.207	3.129	1.071	5.315
14T	0.824	0.015	0.028	0.051	1.052	5.122
14S	0.835	0.041	0.075	0.401	1.052	5.255
14D	0.803	0.018	0.033	0.081	1.007	5.222
15T	0.887	0.020	0.037	0.094	1.140	5.034
15S	0.830	0.168	0.309	7.538	1.029	5.497
15D	0.834	0.170	0.313	7.408	1.014	5.703
16T	0.869	0.022	0.041	0.112	1.079	5.353
16S	0.771	0.024	0.044	0.169	0.938	5.712
16D	0.838	0.025	0.046	0.169	1.010	5.812
17T	0.986	0.115	0.211	0.969	1.320	4.433
17S	0.662	0.119	0.220	2.394	0.852	5.017
17D	0.850	0.068	0.126	0.921	1.081	5.291
18T	0.652	0.264	0.487	2.726	1.016	2.231
18S	0.628	0.128	0.236	0.862	0.953	2.627
18D	0.615	0.361	0.665	7.235	0.927	2.740
ICWW	0.256	3.102	5.651	220.5	0.404	0.683

## Summary and Conclusions

The wind tidal flat area of the Laguna Madre, Texas is a modern marine, quartz sand based, coastal sabkha. Two major types of water masses are observed within this system. The first type, observed only in the basin area, is most likely continental in origin. It charcteristically has a lower percentage of sulfate, and a higher Cl/Br and lower Mg/Ca molar ratio, than the other major water mass. Input of this water mass into the basin area is most likely in response to a regional hydrostatic head rather tha evaporative pumping. The second type of water mass is a Na-Cl brine depleted in Ca with respect to sea water. Molar ratios of the conservative ions indicate that the Laguna Madre is the source for this water mass. Variations in Laguna Madre composition are reflected in the slight variability in brine conservative ion molar ratios. Using bromide as a conservative indicator, brine salinities range from 2 to 9 times that of sea water. The major geochemical mechanism effecting brines in the study area is evaporitic concentration with subsequent precipitation of calcium carbonate and calcium sulfate minerals. Solute fractionation of potassium occurs to a minor degree in the area Brine mixing is localized to the basin area at depth, and between the Na-Cl brines and the freshwtaer lenses of Padre Island and the smaller islands within the area The area of mixing between the Laguna Madre derived brines and the continentally derived brines occurs westward or at a depth greater than 3.8 meters.

Flood recharge and not evaporative pumping is the major hydrological process operating within the study area. Water input

into the sabkha occurs by periodic flooding. This flood water undergoes partial evaporation and seeps into the sediment as salt fingers where additional evaporation modified its chemisty. Flooding is a function of wind direction, wind velocity, surface elevation, and distance from source waters. Therefore, the chemical composition of the interstitial waters is a function of the amount of flooding at the site and the amount of evaporation, which in turn are governed by the climatic, sedimentological and geomorphological characteristics of the Laguna Madre sabkha.



#### BIBLIOGRAPHY

- Adams, J. E., and Rhodes, M. L., 1960, Dolomitization by seepage refluxion: Am. Assoc. Petroleum Geologists Bull., v. 44,p. 1912-1920.
- Amdurer, M., 1978, Geochemistry, hydrology, and mineralogy of the Laguna Madre Flats, South Texas (unpub. Masters thesis): Univ. of Texas, Austin. 172 p.
- Amdurer, M., Munson, M. G. and Salvatore, V.Jr., 1979, Depositional history and rate of deposition of a flood-tidal delta, Central Texas coast: Contrib. in Marine Science, v.22, p. 205-214.
- Badiozamani, K., 1973, The Dorag dolomitization model-application to the middle Ordovician of Wisconsin: Jour. Sed. Petrology, v. 43, p. 965-984.
- Brown, E., Skougstad, M. W. and Fishman, M. J., 1970, Methods for collection and analysis of water samples for dissolved minerals and gases: Techniques of Water-Resources Investigations of the United States Geological Survey, Chapter Al, Book 5, 160 p.
- Bush, P., 1973, Some aspects of the diagenetic history of the sabkha in Abu Dhabi, Persian Gulf, p. 395-407: in Purser, B. H., (ed.), The Persian Gulf: Springer, Berlin, 471 p.
- Butler, G. P., 1969, Modern evaporite deposition and geochemistry of coexisting brines, the sabkha, trucial coast, Arabian Gulf: Joursed. Petrology, v. 39, p. 70-89.
- Carpenter, A. B., 1978, Origin and chemical evolution of brines in sedimentary basins: Oklahoma Geological Survey. Cir. 79, p. 60-77.
- Davis, S. N. and DeWiest, R., 1966, Hydrogeology: John Wiley and Sons, New York, 463 p.
- Deffeyes, K. S., Lucia, F. J. and Weyl, P. K., 1965, Dolomitization of recent and Plio-Pleistocene sediments by marine evaporite waters on Bonaire, Netherlands, Antilles, p. 71-88: in Dolomitization and Limestone Diagenesis, Soc. Econ. Paleontologists and Mineralogists Spec. Pub. 13.
- de Groot, K., 1973, Geochemistry of tidal flat brines at Umm Said, SE Qatar, Persian Gulf, p. 377-394: in Purser, B. H. (ed.), The Persian Gulf, Springer, Berlin, 471 p.

- Dunk, R., Mostyn, R. A. and Hoare, H. C., 1969, The determination of sulfate by indirect atomic absorption spectroscopy: Atomic Absorption Newsletter, v. 8., no. 4, p. 79-81.
- Eugster, H. P. and Jones, B. F., 1979, Behavior of major solutes during closed-basin brine evolution: Amer. Jour. Science, v. 279, p. 609-631.
- Evans, G. and Shearman, D. J., 1964, Recent celestite from the sediment of the Trucial coast of the Persial Gulf: Nature, v. 202, p. 385-386.
- Evans, G., Kendall, C. G. and Skipwith, Sir. P., 1964, Origin of the coastal flats, the sabkha, of the Tricial coast, Persian Gulf: Nature, v. 202, p. 579-600.
- Evans, G., Murray, J. W., Biggs, H.E.J, Bate, R. and Bush, P. R., 1973, The oceanography, ecology, sedimentology, and geomorphology of parts of the trucial coast barrier island complex, Persian Gulf, p. 233-278: in Purser, B. H. (ed.), The Persian Gulf, Springer, Berlin, 471 p.
- Fisk, H. N., 1959, Padre Island and the Laguna Madre flats coastal south Texas: Coastal Studies Inst., Second Coastal Geography Conf., Louisiana State Univ., p. 103-151.
- Friedman, G. M. and Sanders, J. E., 1967, Origin and occurrence of dolostones: in Chilingar, G. V., Bissell, H. J., and Fairbridge, R. W. (eds.), Carbonate rocks: origin, occurrence and classification: Developments in Sedimentology, Elsevier, Amsterdam, v. 9A, p. 267-348.
- Garrels, R. M. and Christ, C. L., 1965, Solutions, Minerals, and Equilibria, Freeman, Cooper and Co, San Francisco, 450 p.
- Garrels, R. M. and Thompson, M. E., 1962, A chemical model for sea water at 25°C and one atmosphere total pressure: Amer. Jour. Science. v. 260,p. 57-66.
- Goldberg, E., 1963, Chemistry-the oceans as a chemical system, McGraw Hill, M. N. (ed.), Composition of sea water, comparative and descriptive oceanography, Vol. II of the Sea, Interscience, New York, p. 3-25.
- Grim, R. E., 1968, Clay Mineralogy, McGraw-Hill, New York, 596 p.
- Hahl, D. C., and Ratzlaff, K. W., 1972, Chemical and physical p. characteristics of water in estuaries of Texas: October 1968-September 1969, Texas Water Development Board Report, Austin, 144
- Hahl, D. C., and Ratzlaff, K.W., 1975, Chemical and physical characteristics of water in estuaries of Texas: October 1970 September 1971, Texas Water Development Board Report, Austin, 191

- Helgeson, H. C., 1969, Thermodynamics of hydrothermal systems at elevated temperatures and pressures, Amer. Jour. Science, v. 267, p. 729-804.
- Horne, R. A., 1969, Marine Chemistry: Wiley-Interscience, New York, 568 p.
- Hsu, K. J. and Siegenthaler, C., 1969, Preliminary experiments on hydrodynamic movement induced by evaporation and their bearing on the dolomite problem: Sedimentology, v. 12, p. 11-25.
- Hsu, K.J. and Schneider, J., 1973, Progress report on dolomitization-Hydrology of the Abu Dhabi sabkhas, Arabian Gulf, p. 409-422: in Purser, B. H. (ed.), The Persian Gulf, Springer, Berlin, 471 pp.
- Illing, L. V., Wells, A. J. and Taylor, J. C. M., 1965,
  Penecontemporary dolomite in the Persian Gulf: in Pray, L.C. and
  Murray, R. C. (eds), Dolomitzation and limesotone diagenesis,
  S.E.P.M., Spec. Pub. 13, p. 89-111.
- Jones, B. F., Eugster, H. P. and Rettig. S. L., 1977, Hydrochemistry of the Lake Magadi Basi, Kenya: Geochim. et Cosmochim. Acta., v. 41, p. 53-72.
- King, R. H., 1947, Sedimentation in Permian Castile Sea: Am. Assoc. Petroleum Geologists Bull. v. 31, p. 470-477.
- Kinsman, D. J., 1964, The recent carbonate sediments near Halat el Bahrini, Trucial coast, p. 185-192: in Van Troaten, L.M.J.U. (ed.), Deltaic and Shallow Marine Environments, Developments in Sedimentology, v. 1, Elsevier, Amsterdam.
- Kinsman, D. J., 1966, Gypsum and anhydrite of recent age, Trucial coast, Persian Gulf, p. 302-326: in Rau, J.L. (ed.), Proc. Second Salt Symp., Publ. Northern Ohio Geol. Soc., v. 1, p. 26.
- Kinsman, D. J. J., 1969, Modes of formation, sedimentary associations, and diagnostic features of shallow-water and supratidal evaporites: Am. Assoc. Petroleum Geologists Bull., v. 53, p. 830-840.
- LeBlanc, R.J. and Hodgson, W. D., 1959, Origin and development of the Texas shoreline: Coastal Studies Inst., Second Coastal Geography Conf., Louisiana State Univ, p. 57-101.
- Levy, Y., 1977a, The origin and evolution of brine in coastal sabkhas, Northern Sinai: Jour. Sed. Petrology, v. 47, p. 451-462.
- Levy, Y., 1977b, Description and mode of formation of the supratidal evaporite facies in Northern Sinai coastal plain: Jour. Sed. Petrology, v. 47, p. 463-474.

- Lind, W. B., 1979, Chemical and physical characteristics of water estuaries of Texas: October 1973-September 1974, Texas Dept. of Water Resources Report, Austin, 231 pp.
- Masson, P. H., 1955, An occurrence of gypsum in southwest Texas: Jour. Sed. Petrology, v. 25, p. 72-77.
- McKenzie, J. A., Hsu, K. J., and Schneider, J. F., 1980, Movement of subsurface waters under the sabkha, Abu Dhabi, UAE. and its relation to evaporative dolomite genesis: in Zenger, D. H. and others (eds.), Concepts and Models of Dolomitization, S.E.P.M., Spec. Pub. 28, p.11-30.
- National Oceanic and Atmospheric Administration, 1979, Climatological Data, Annual summary, Texas: National climatic Center, Asheville, North Carolina, v. 84.
- National Oceanic and Atmospheric Administration, 1980, Climatological Data, Annual Summary, Texas: National Climatic Center, Asheville, North Carolina, v. 85.
- Patterson, R. J. and Kinsman, D. J. J., 1977, Marine and Continental groundwater sources in a Persian Gulf coastal sabkha: Am. Assoc. petroleum Geologists Studies in Geology, No. 4, p. 381-397.
- Phleger, F. B., 1969, A modern evaporite deposit in Mexico, An. Assoc. Petroleum Geologists Bull, v. 53, p. 824-829.
- Presley, B. J., 1971, Part 1: Determination of selected minor and major inorganic constituents: in Eving, J. I., and others (eds.), Initial reports of the deep sea drilling project, volume VII, Washington, U. S. Govt. Print. Off, p. 1749-1755.
- Price, W. A., 1933, Role of diastrophism and topography of Corpus Christi area, South Texas: Am. Assoc. Petroleum Geologists Bull., v. 17, p. 907-967.
- Price, W. A., 1947, Equilibrium of form and forces in tidal basins of coast of Texas and Louisiana: Am. Assoc. Petroleum Geologists Bull., v. 31, p. 1619-1663.
- Price, W. A., 1958, Sedimentology and Quaternary geomorphology of South Texas: Gulf Coast Assoc. Geol. Soc. Trans., v. 8, p. 41-75.
- Ratzlaff, K. W., 1976, Chemical and physical characteristics of water in estuaries of Texas: October 1971 - September 1973, Texas Water Development Board Report, Austin, 208 p.
- Raup, O. B., 1970, Brine mixing, An additional mechanism for formation of basin evaporites: Am. Assoc. Petroleum Geologists Bull., v. 54, p. 2246-2259.

- Rawson, R. R., 1976, Sabkha Environment: New frontiers for uranium exploration: Am. Assoc. petroleum Geologists. Bull., v. 60, p. 1406-1407.
- Renfro, A.R., 1974, Genesis of evaporite-associated stratiform metalliferous deposits A sabkha process: Econ. Geology, v. 69, p. 33-45.
- Rouse, J. E., and Sherif, N., 1980, Major evaporite deposition from groundwater remobilized salts: Nature, v. 285, p. 470-472.
- Runnells, D. D., 1969, Diagenesis, chemical sediments, and the mixing of natural waters: Jour. Sed. Petrology, v. 39, p. 1188-1201.
- Rusnak, G.A., 1960, Sediments of Laguna Madre, Texas, p. 153-196: in Shepard, R. P. and others (eds), Recent sediments, Northwestern Gulf of Mexico, Am. Assoc. Petroleum Geologists, Tulsa, 394 p.
- Shafer, G. H., and Baker, E. T., 1973, Ground-water resources of Kleberg, Kenedy, and Southern Jim Wells counties, Texas: July 1973, Texas Water Development Board Report, Austin, 58 p.
- Shearman, D. J., 1963, Recent anhydrite, gypsum, dolomite and halite from the coastal flats of the Arabian shore of the Persian Gulf, Proc. Geol. Soc. Lond., v. 63.
- Stumm, W. and Morgan, J. J., 1970, Aquatic Chemistry, Wiley-Interscience, New York, 583 p.
- Truesdell, A. H. and Jones, B. F., 1973, WATEQ, a computer program for calculating chemical equilibria of natural waters: Nat. Tech. Information Service Rept., p. 220-464, U. S. Dept. of Commerce, Springfield, Va.
- Valyashko, M. G., 1956, Geochemistry of bromine in the process of salt deposition and the use of the bromine content as a genetic and prospecting criterion, Geochemistry, v. 6, p. 570-589.
- Van Andel, T.H. and Poole, D. M., 1960, Sources of recent sediments in the northern Gulf of Mexico, Jour. Sed. Petrology, v. 30, p. 91-122.
- Weast, R. C. (ed.), 1979, Handbook of chemistry and physics, CRC Press, Boca Raton, Florida, 2347 pp.
- West, I. M., Ali, Y. A., and Hilmy, M. E., 1979, Primary gypsum nodules in a modern sabkha on the Mediterranean coast of Egypt: Geology, v. 7, p. 354-358.
- Wigley, T.M. L. and Plummer, L. N., 1976, Mixing of carbonate waters: Geochim et Cosmochim. Acta. v. 40, p. 989-995.

- Wilkinson, B. H., 1975, Matagorda Island, Texas: the evolution of a gulf coast barrier complex: Geol. Soc. American Bull., v. 86, p. 959-967.
- Zherebtsova, I. K. and Volkova, N. N., 1966, Experimental study of behavior of trace elements in the process of natural solar evaporation of Black Sea water and Sasyk-Sivash brine: Geochemistry International, v. 3, p. 656.670.

Appendix A

Sulfate analysis

Sulfate analysis was conducted indirectly by atomic absorption using a modification of the technique proposed by Dunk et al. (1969). In this method a known quantity of barium, in excess of sulfate to be analysed, is added to the samples and prepared sulfate standards. This barium reacts with the sulfate and precipitates out as barium sulfate. Sulfate is determined indirectly by measuring the remaining quantity of barium in solution of the samples and standards by A.A. Errors due to variations in time and temperatures for this reaction to go to completion and to the partial solubility of the precipitated barium sulfate are eliminated by the use of sulfate standards similarly treated (Dunk et al., 1969). All samples were diluted 1/100 before analysis because of the large amount of sulfate in the samples. Also a barium standard of greater concentration than that proposed by Dunk et al. (1969) had to be used. In the procedure 25 ml of the diluted sample is added to 25 ml of a 750 mg/l standard solution of barium. The solution is mixed followed by addition of 1 ml of 100 g/l potassium solution and two drops of concentrated HCl. This solution is then premitted to react overnight before analysis.

A slightly acidic solution is needed to have a more complete reaction between the barium and sulfate. A 2000 mg/l matrix of potassium was needed to suppress ionization during Ba analysis by A.A. Since this addition of potassium was one of the modifications done to the Dunk et al. (1969) technique, two equivalent standards of sulfate were prepared with the only difference being the presence of potassium. Analysis revealed that this potassium matrix has no significant effect on the reactions between barium and sulfate. A linear relationship exists between barium absorbance and sulfate

concentrations. Therefore, a linear regression analysis on the barium absorbance of the standard versus the sulfate concentrations then enables one to determine the sulfate concentration of the samples. This method provides a precision of better than 5.0% (2 std. deviations).

Appendix B

Bromide Analysis

The technique used in bromide analysis is a modification of that proposed by Presley (1971). In this method bromide is oxidized with chloramine—T (sodium paratoluene—sulfonchloramine) and the resultant color change is measured spectrophotometrically at 595 millimicrons. Modifications were necessary because of the higher concentrations of bromide in the samples and the large differences in bromide content between samples. Modifications included increasing the amount of chloramine—T, acetate—buffer, and sodium thiosulfate used. Preliminary experiments using 0 ppm, 10000 ppm, and 20000 ppm chloride matrixes in the bromide standards indicate that chloride concentrations have negligible effects on the oxidation of bromide as well as the measured transmittance of the standards.

The reagents used were chloramine-T, acetate buffer, phenol red and sodium acetate. These reagents were prepared in accordance to the method prescribed by Presley (1971). Bromide standards between 0 and 70 ppm, at 10 ppm intervals, were also prepared.

In this procedure 0.1 ml of sample, or 1.0 ml of standard, is first added to a 25 ml solution of phenol red-acetate buffer. Then 4 ml of chloramine-T is added to this solution and allowed to react for thirty seconds. The larger amount of chloramine-T was needed in order to oxidize the greater amount of bromide in the samples. After thirty seconds 10 ml of sodiumthiosulfate solution is added to stabilize the solution. Because of the greater amount of bromide and chloramine-T in solution a larger amount of sodiumthiosulfate was also needed. The time the solution was allowed to react was not modified because preliminary experiments indicated no need for this.

A plot of brimide concentration versus transmittance has been

found to have a linear relationship for a limited range of bromide concentrations. A linear regression analysis within this range generates a correlation coefficient of less than -0.998 (approaching -1.0). The concentrations of bromide that lie on this linear line and the slope of the line are a function of the amount of phenol red-acetate buffer solution used. In Figure 16, the upper curve represents and average curve generated during sample analysis. linear range is for a 20 to 60 ppm bromide concentration. The lower curve was generated using a 15 ml phenol red-acetate buffer solution. It is evident that increasing the amount of this solution will result in a linear realationship between bromide concentration and transmittance at higher bromide values. However, some sacrifice in precision results because of the decrease in slope of the line. was minimized by the generation of new working curves for each suite of samples analysed. This resulted in a 1.8 percent precision (2 standard deviations).

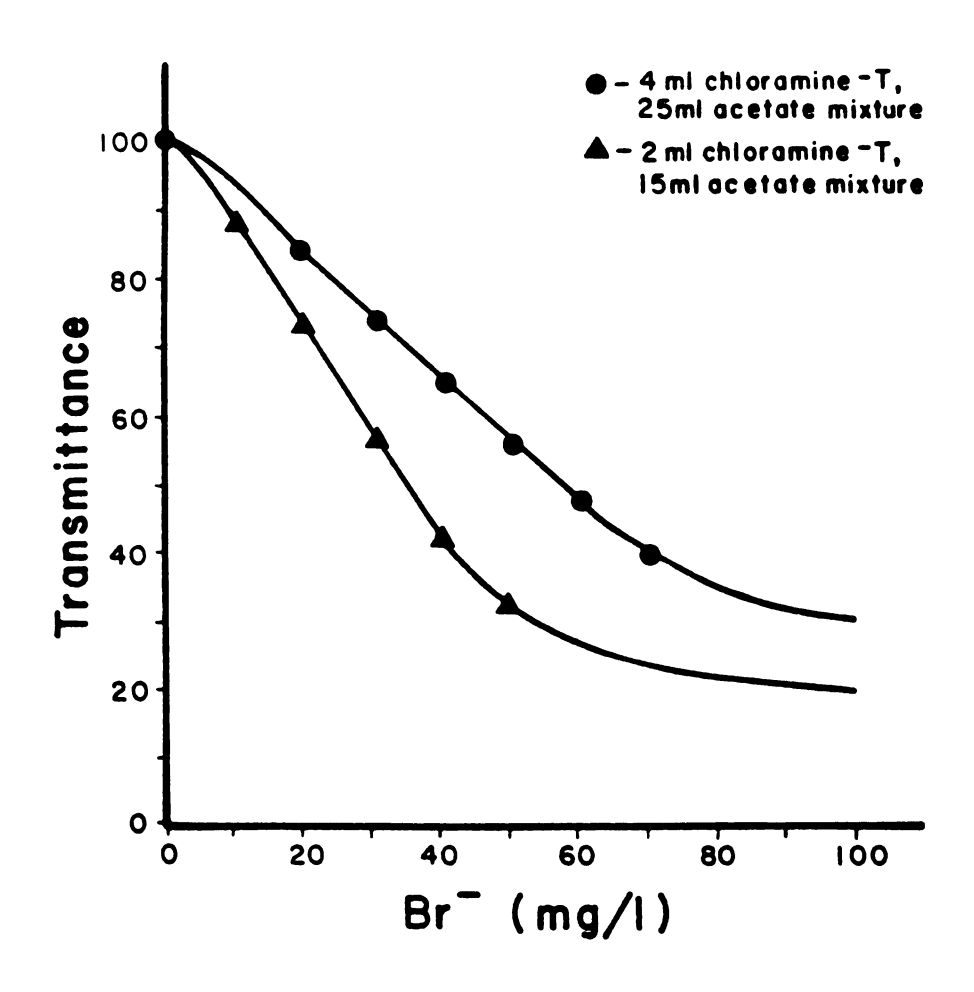


Figure 16. Bromide vs. Transmittance.

Appendix C

Density Measurements

In order to chemically model the Laguna Madre system and to determine the piezometric potentials at each sample site, brine densities must be known. The density of water varies with temperature; therefore, field temperature must be considered when determining sample densities. Water temperatures in the field ranged from 20.5°C to 34.0°C. The density of pure water, which is effected the least by temperature changes (Fig. 17), would have a 3.7 mg (0.4%) change over this temperature range.

Density measurements were performed in the laboratory using a 10 ml pycnometer and an analytical balance. Sample temperatures never equalled field temperatures; therefore, a technique was developed to convert the measured densities to field densities.

A plot of water temperature versus density (Fig. 17) indicates that, although the density variation with temperature is similar at different salinities, it is not identical. The lines in Figure 17 represent different salinities at increasing temperatures. However, a 10°/00 increase in salinity at a specific temperature will result in a constant increase in density, regardless of its original salinity. For example at 32°C (Fig. 17) the difference in water density between 0 and 10°/00 equals the difference in density between 30 and 40°/00. Therefore, at a constant temperature, the relationship between density and salinity is linear (Fig. 18) and has a correlation coefficient greater than 0.99998. The slope and y intercept of the line representing this relationship (Fig. 18) is a function of temperature. The relationship between density, temperature and salinity is shown in Figure 19. The data used to generate these

figures was taken from Horne (1969). In Figure 17, the y intercept of each temperature line represents the density of pure water at that temperature. The relationship of pure water density with temperature has been defined by the following equation:

density 
$$(g/cm^3) = (999.83952 + 16.945176 t - 7.9870401 x 10^{-3}t^2 - 46.170461 x 10^{-6} t^3 + 105.56302 x 10^{-9} t^4 - 280.54253 x 10^{-12} t^5) / (1 + 16.87985 x 10^{-3} t) x 1000$$

(1)

(Weast, 1979, p. F-6). The variation in slope of each temperature line (Fig. 18) is characterized by the following equation:

slope = 
$$8.300245 \times 10^{-4} - 2.2274915 \times 10^{-5} \ln t$$
 (2)

this equation was derived from the data obtained from Horne (1969) and has a correlation coefficient greater than 0.996.

With these two equations it is possible to determine the density of a water sample at another temperature. The procedure used to determine sample densities at field temperatures is as follows:

(a) Given a measured density and temperature an equation is derived for the density versus salinity line (Fig. 18). The y intercept is determined from equation (1) and the slope is determined from equation (2).

$$\frac{\text{density - y intercept}}{\text{slope}} \tag{3}$$

(b) To determine the density at a new temperature, the line representing density versus temperature at this new temperature is generated. The new y intercept and new slope are also determined from equations (1) and (2). Salinity (g/kg) is not a function of temperature; therefore, this remains constant. The density at the new temperature is related by the following equation:

density' = salinity x slope ' + y intercept ' (4)

where salinity, slope and y intercept at the new temperature are known.

There are two possible sources of error that can occur from this technique. The first is in computing the change in line slope (Fig. 18) with temperature. However, since field temperatures lie between 0-40°C, the range measured by Horne (1969), this source of error is minor. The second source of error could be the lack of experimental data at high salinities. The line representing density versus salinity is linear; however, this relationship has not been proved to be consistent at high salinities.

In order to evaluate these problems the densities of different brines at various temperatures were measured. This was done by first placing the sample in the pycnometer and weighing it. The sample and pycnometer are then placed in the oven and heated slightly. After a few seconds the sample is removed from the oven, the temperature is measured and the water that ran out of the pycnometer is wiped off. This technique was repeated often using the same sample and a variation of less than 0.01% was measured. Table 6 is a comparison using equation (1-4) at these temperatures. The largest deviation of predicted versus measured densities is 0.2 mg. This error, assuming no error in laboratory measurements of densities, is less than 0.02%. The experimental data is limited and should be expanded to properly evaluate this technique; however, a 0.0003 g error in predicted densities would be a safe estimate in chemically modelling the waters and determining sample site piezometric potentials.

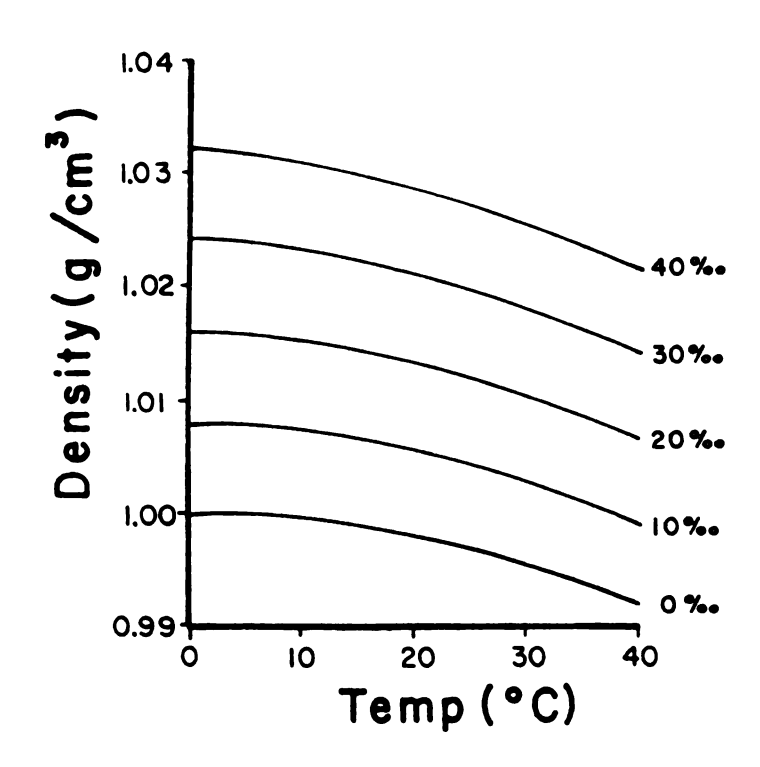


Figure 17. Density vs. Temperature.

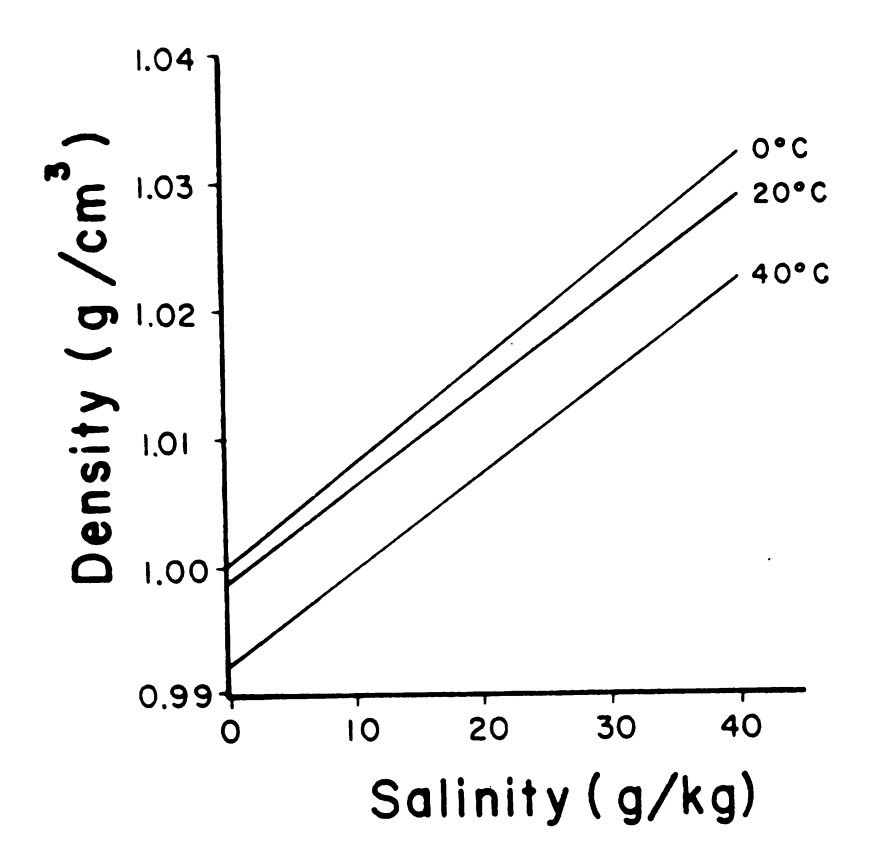


Figure 18. Density vs. Salinity.

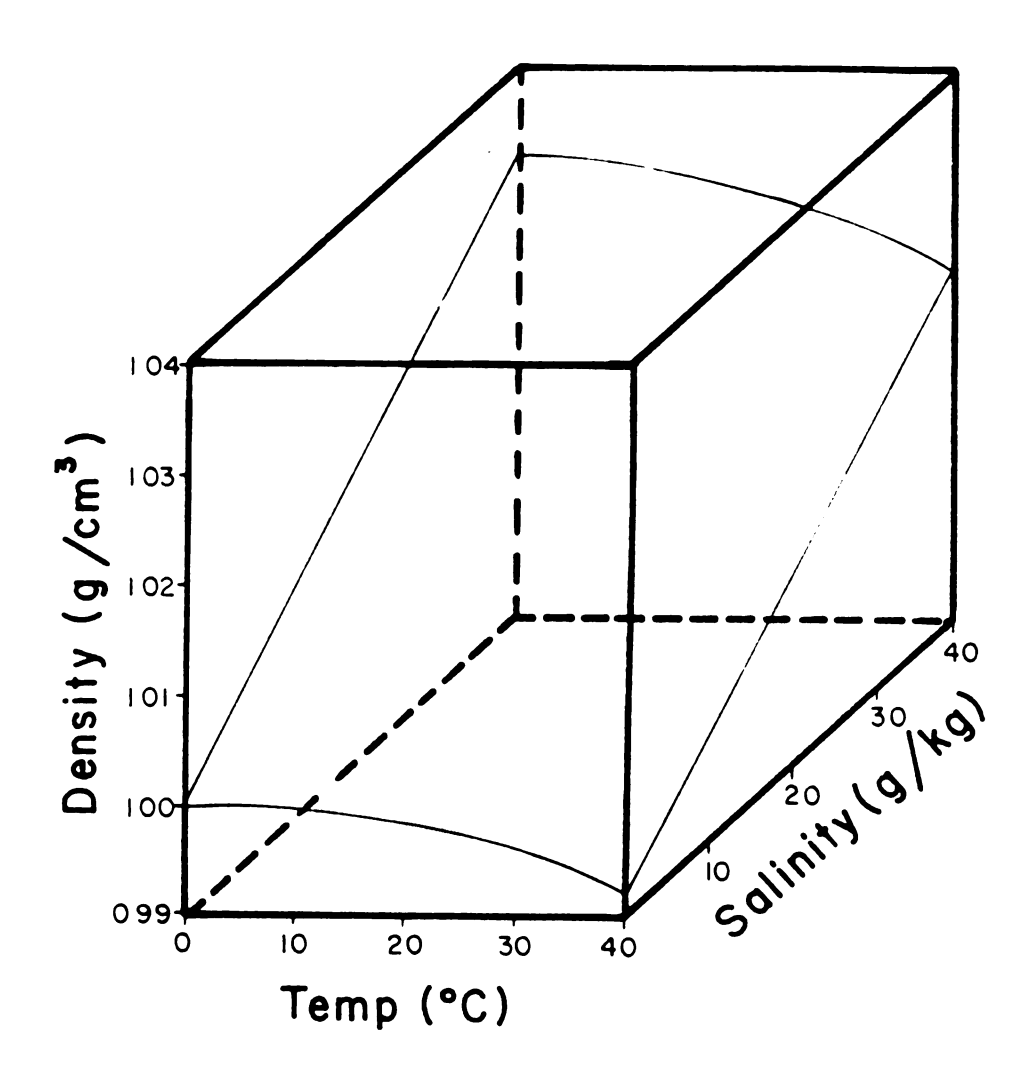


Figure 19. Density vs. Temperature vs. Salinity.

Table 6

Laboratory Density Measurements

Sample	Temp(°C)	measured density(g/cm <sup>3</sup> )	<pre>predicted density(g/cm<sup>3</sup>)</pre>	measured - predicted
12D	25.5	1.17787	1.17789	-0.00002
	28.7	1.17638	*	
	30.5	1.17559	1.17552	+0.00007
	32.2	1.17477	1.17470	+0.00007
	33.2	1.17425	1.17421	-0.00004
<b>9</b> S	27.5	1.11427	1.11431	-0.00004
	30.0	1.11328	*	
	31.7	1.11244	1.11256	-0.00012
	32.8	1.11206	1.11209	-0.00003
	33.9	1.11141	1.11161	-0.00020
ICWW	24.2	1.02571	1.02551	+0.00020
	29.2	1.02399	*	
	32.2	1.02299	1.02299	0.00000
	35.7	1.02177	1.02173	+0.00004
	38.0	1.02099	1.02085	+0.00014

<sup>\*</sup> Measured density at this temperature was used to generate salinity.

Appendix D

Analysis

-103-August Analysis

Well	Temp	pН	density	y Ca	Mg	Na	K	C1	so <sub>4</sub>	HCO.	3 <sup>Sr</sup>	Br
9T	29.0	6.60	1.1101	1080	6300	49300	1550	88662	11952	400	20	310
8T	32.0	7.20	1.1225	970	7200	56600	1630	101950	11952	400	20	310
AMlT	32.0	7.08	1.1179	970	7000	57700	1750	102605	13475	253	21	329
CAM 2	34.0*	8.28	1.0230	560	1300	1260	300	22028	3206	155	8	68.9
7T	22.0	6.68	1.1400	990	7600	66700	1870	118638	13142	230	17	405
6T	31.0	6.40	1.1309	850	6900	61200	1870	108398	12300	258	17	384
5T	32.0	6.55	1.1324	810	8200	60600	1930	109222	15141	263	20	342
4T	32.0	6.50	1.1239	930	7000	53600	1640	96697	12643	<b>3</b> 0 <b>3</b>	18	367
3T	32.0	6.40	1.1240	820	7000	54100	1570	96333	13842	290	22	351
2T	22.0	7.05		1400	1600	13900	370	25327	4344	655	17	67.8
ICWW	34.0*	8.20	1.0202	440	1100	11500	270	2020 <b>9</b>	2281	125	5	59.8
13T	33.0	6.85	1.1505	670	9100	66800	2160	119575	17456	295	20	423
1 2T	33.0	6.50	1.1634	490	10400	77100	2230	137666	19473	135	14	489
11 <b>T</b>	34.0	6.60	1.1488	530	9400	70900	2020	124784	19784	230	14	413
14T	32.0			540	11100	82300	2282	147919	19274		20	
15T	32.5	6.90	1.1654	470	10900	<b>75200</b>	2370	135535	20472	157	15	511
16T	32.5	6.80	1.1705	520	10600	81700	2410	146812	17807	95	16	515
17T	30.0	6.80	1.1367	770	6800	72800	2200	127753	10310	160	24	399
18T	31.0*	7.05	1.0658	780	<b>37</b> 00	30000	910	54117	6806	205	26	186
9S	32.0*	7.10	1.1147	870	7000	53200	1580	96388	11952	365	25	320
8S	32.0*	6.88	1.1144	990	6900	51600	1460	93360	12472	355	23	338
AM1S	31.0*	7.03	1.0630	960	<b>3</b> 500	29300	900	51227	8875	220	15	154
<b>7</b> S	33.0*	7.15	1.1272	920	7000	61300	1860	109988	10972	300	29	371
6S			1.1353					120573				
5S	-		1.1357	740				115766				
48			1.1252					108480				
<b>3</b> S			1.1286	870				113631				
13S			1.1437					128992				
12S			1.1694					136833				
118			1.1692									
148			1.1715									
			1.1750	420				142971				
16S	32.0	6.80	1.1803	430	8700	89500	2680	151867	19883	70	11	564

## August Analysis (continued)

Well

	Temp	pН	density	y Ca	Mg	Na	K	C1	so <sub>4</sub>	нсо.	Sr	Вr
17S									·			
18 <b>S</b>	31.0	6.80	1.1495	640	8100	76000	<b>2</b> 500	134153	13500	183	18	464
<b>9</b> D	30.0	7.05	1.0851	690	4300	41500	1310	72628	8396	210	50	242
8D	33.0*	6.75	1.1134	990	6900	58600	1560	104611	11958	<b>3</b> 80	21	335
AM1D	33.0*	6.70	1.1150	1460	<b>73</b> 00	58400	1400	106496	11505	368	19	329
<b>7</b> D	31.0*	6.90	1.0834	750	4600	<b>39</b> 800	1230	67787	12642	200	12	209
6D	33.0*	6.65	1.1261	1070	7600	60600	1780	110321	11616	395	25	397
5D	33.0	6.45	1.1265	990	8000	58800	1520	108012	12010	450	25	378
4D	32.0	6.50	1.1402	790	8100	<b>7</b> 0700	2050	124871	14637	400	25	429
2D	32.0	6.50	1.1352	960	8200	65400	1530	118514	12301	450	28	<b>39</b> 0
13D	33.0	6.60	1.0854	1080	5500	38800	1050	71019	10074	486	20	228
12D	32.0	6.50	1.1423	<b>9</b> 20	8100	72800	2060	130726	11491	305	17	427
11D	33.0	6.85	1.1715	520	12500	80700	2560	148721	20693	260	13	536
14D	32.0	6.85	1.1697	550	11800	79100	2390	144035	20639	460	13	507
15D	34.0	6.70	1.1725	510	12100	82100	2590	150166	20179	150	12	526
16D	34.0	6.73	1.1764	550	12500	85900	2670	158087	18973	390	12	561
17D	34.0*	6.65	1.1836	490	11600	87200	2640	156630	20139	120	11	578
18D	31.0	6.80	1.1674	600	10700	79400	2620	143865	17782	168	12	515
10 <b>T</b>	30.0	7.10	1.0890	790	5100	42900	1330	77492	8144	225	47	267
AM 5T	30.0	6.80	1.1004	1100	5400	46700	1390	82896	10434	645	28	283
AM4T	31.0	6.65	1.0920	1120	4600	43900	1220	79559	5956	425	23	262
AM 3T	31.5	6.65	1.1135	1090	6400	57300	1600	102305	10643	425	23	317
AM2T	31.0	<b>6.7</b> 0	1.0700	930	3400	34900	970	62733	4134	820	18	196
10 <b>s</b>	31.0*	6.70	1.1031	1040	6100	49800	1470	89944	10245	438	21	295
AM 5S	32.0*	6.45	1.1057	1530	5700	49800	1510	90599	9043	385	30	305
AM4S	31.0*	7.13	1.0328	690	1700	17400	440	30664	3449	345	11	57.6
AM3S	31.0*	6.68	1.0570	1010	3100	28000	780	52355	2843	450	16	144
AM2S	31.0*	7.03	1.0303	940	1700	15800	380	27983	4134	511	13	64.1
10D	31.0*	6.70	1.0258	740	1400	13400	350	23769	3393	175	11	54.3
AM 5D	33.0*	6.48	1.1018	1270	5200	49000	1460	87942	8311	385	28	305
AM4D	31.0*	6.60	1.0894	1660	4500	42300	1290	78119	5621	335	35	239
AM 2D	31.0*	6.68	1.0769	1570	3700	36200	<b>9</b> 50	68240	2151	735	31	212
	31.0*	<b>7.</b> 50	1.0368	940	2100	1880	480	33384	4979	268	13	70.7

## March Analysis

9T
8T       21.0       6.55       1.1128       1190       6820       54500       1330       98628       11470       264       16       326         AMIT       23.0*       6.70       1.1203       950       8000       55700       1600       105000        186       18       362         CNAL       22.0       8.15       1.0259       680       1330       11200       310       19992       3469       142       9       65.9         7T       21.5       6.40       1.1411       1080       8060       69400       1970       124680       12757       225       17       447         6T       21.0       6.40       1.1382       1130       7760       66900       1790       122681       13829       192       15       452         4T       21.8       6.65       1.1322       1120       7880       65700       1630       119023       11684       192       17       417         3T       21.8       6.20       1.1322       1120       7880       65700       1630       119023       11684       192       17       417         3T       21.0       6.20       1.132
AMIT 23.0* 6.70 1.1203 950 8000 55700 1600 105000 186 18 362 CNAL 22.0 8.15 1.0259 680 1330 11200 310 19992 3469 142 9 65.9 7T 21.5 6.40 1.1411 1080 8060 69400 1970 124680 12757 225 17 447 6T 21.0 6.40 1.1382 1130 7760 66900 1790 120969 11255 249 19 437 5T 22.0 6.65 1.1394 910 8430 68100 1970 122681 13829 192 15 452 4T 21.8 6.20 1.1322 1120 7880 65700 1630 119023 11684 192 17 417 3T 21.0 6.10 1.1356 1000 8720 63800 1670 117055 13400 269 14 410 2T 20.5 7.08 1.0308 1270 1820 12600 370 24392 3535 550 14 48.0 1000 1000 1000 1000 1000 1000 1000 1
CNAL 22.0 8.15 1.0259 680 1330 11200 310 19992 3469 142 9 65.9  7T 21.5 6.40 1.1411 1080 8060 69400 1970 124680 12757 225 17 447  6T 21.0 6.40 1.1382 1130 7760 66900 1790 120969 11255 249 19 437  5T 22.0 6.65 1.1394 910 8430 68100 1970 122681 13829 192 15 452  4T 21.8 6.20 1.1322 1120 7880 65700 1630 119023 11684 192 17 417  3T 21.0 6.10 1.1356 1000 8720 63800 1670 117055 13400 269 14 410  2T 20.5 7.08 1.0308 1270 1820 12600 370 24392 3535 550 14 48.0  ICWW 24.5 8.18 1.0259 440 1366 11100 300 19795 3072 154 6 62.1  13Ts 24.0 6.60 1.1568 720 10130 77300 1940 138964 17260 135 18 486  13Td 22.0 6.80 1.1513 720 9740 77700 1860 90000 16 421  Dayl 29.5* 1.1048 1450 6470 48400 1500 88150 12420 24 313  Day2 29.5 7.50 1.1248 1170 8600 59500 1730 109099 15205 266 28 382  12T 20.5 7.10 1.1696 710 11750 79300 2080 144655 20263 154 13 526  11T 21.5 6.70 1.1526 670 10650 74700 1870 134610 19619 79 13 455  14T 21.5 6.30 1.1704 570 12200 77100 2110 143799 18333 89 11 535
7T       21.5       6.40       1.1411       1080       8060       69400       1970       124680       12757       225       17       447         6T       21.0       6.40       1.1382       1130       7760       66900       1790       120969       11255       249       19       437         5T       22.0       6.65       1.1394       910       8430       68100       1970       122681       13829       192       15       452         4T       21.8       6.20       1.1322       1120       7880       65700       1630       119023       11684       192       17       417         3T       21.0       6.10       1.1356       1000       8720       63800       1670       117055       13400       269       14       410         2T       20.5       7.08       1.0308       1270       1820       12600       370       24392       3535       550       14       48.0         ICWW       24.5       8.18       1.0259       440       1366       11100       300       19795       3072       154       6       62.1         13Ts       24.0       6.60       1.1568<
6T 21.0 6.40 1.1382 1130 7760 66900 1790 120969 11255 249 19 437  5T 22.0 6.65 1.1394 910 8430 68100 1970 122681 13829 192 15 452  4T 21.8 6.20 1.1322 1120 7880 65700 1630 119023 11684 192 17 417  3T 21.0 6.10 1.1356 1000 8720 63800 1670 117055 13400 269 14 410  2T 20.5 7.08 1.0308 1270 1820 12600 370 24392 3535 550 14 48.0  ICWW 24.5 8.18 1.0259 440 1366 11100 300 19795 3072 154 6 62.1  13Ts 24.0 6.60 1.1568 720 10130 77300 1940 138964 17260 135 18 486  13Td 22.0 6.80 1.1513 720 9740 77700 1860 90000 16 421  Dayl 29.5* 1.1048 1450 6470 48400 1500 88150 12420 14 313  Day2 29.5 7.50 1.1248 1170 8600 59500 1730 109099 15205 266 28 382  12T 20.5 7.10 1.1526 670 10650 74700 1870 134610 19619 79 13 455  14T 21.5 6.70 1.1526 670 10650 74700 1870 1343799 18333 89 11 535
5T       22.0       6.65       1.1394       910       8430       68100       1970       122681       13829       192       15       452         4T       21.8       6.20       1.1322       1120       7880       65700       1630       119023       11684       192       17       417         3T       21.0       6.10       1.1356       1000       8720       63800       1670       117055       13400       269       14       410         2T       20.5       7.08       1.0308       1270       1820       12600       370       24392       3535       550       14       48.0         ICWW       24.5       8.18       1.0259       440       1366       11100       300       19795       3072       154       6       62.1         13Ts       24.0       6.60       1.1568       720       10130       77300       1940       138964       17260       135       18       486         13Td       22.0       6.80       1.1513       720       9740       77700       1860       90000        16       421         Day1       29.5*       7.50       1.1248       1
4T 21.8 6.20 1.1322 1120 7880 65700 1630 119023 11684 192 17 417  3T 21.0 6.10 1.1356 1000 8720 63800 1670 117055 13400 269 14 410  2T 20.5 7.08 1.0308 1270 1820 12600 370 24392 3535 550 14 48.0  ICWW 24.5 8.18 1.0259 440 1366 11100 300 19795 3072 154 6 62.1  13Ts 24.0 6.60 1.1568 720 10130 77300 1940 138964 17260 135 18 486  13Td 22.0 6.80 1.1513 720 9740 77700 1860 90000 16 421  Dayl 29.5* 1.1048 1450 6470 48400 1500 88150 12420 24 313  Day2 29.5 7.50 1.1248 1170 8600 59500 1730 109099 15205 266 28 382  12T 20.5 7.10 1.1696 710 11750 79300 2080 144655 20263 154 13 526  11T 21.5 6.70 1.1526 670 10650 74700 1870 134610 19619 79 13 455  14T 21.5 6.30 1.1704 570 12200 77100 2110 143799 18333 89 11 535
3T 21.0 6.10 1.1356 1000 8720 63800 1670 117055 13400 269 14 410 2T 20.5 7.08 1.0308 1270 1820 12600 370 24392 3535 550 14 48.0 ICWW 24.5 8.18 1.0259 440 1366 11100 300 19795 3072 154 6 62.1 13Ts 24.0 6.60 1.1568 720 10130 77300 1940 138964 17260 135 18 486 13Td 22.0 6.80 1.1513 720 9740 77700 1860 90000 16 421 Dayl 29.5* 1.1048 1450 6470 48400 1500 88150 12420 24 313 Day2 29.5 7.50 1.1248 1170 8600 59500 1730 109099 15205 266 28 382 12T 20.5 7.10 1.1696 710 11750 79300 2080 144655 20263 154 13 526 11T 21.5 6.70 1.1526 670 10650 74700 1870 134610 19619 79 13 455 14T 21.5 6.30 1.1704 570 12200 77100 2110 143799 18333 89 11 535
2T       20.5       7.08       1.0308       1270       1820       12600       370       24392       3535       550       14       48.0         ICWW       24.5       8.18       1.0259       440       1366       11100       300       19795       3072       154       6       62.1         13Ts       24.0       6.60       1.1568       720       10130       77300       1940       138964       17260       135       18       486         13Td       22.0       6.80       1.1513       720       9740       77700       1860       90000         16       421         Day1       29.5*        1.1048       1450       6470       48400       1500       88150       12420        24       313         Day2       29.5       7.50       1.1248       1170       8600       59500       1730       109099       15205       266       28       382         12T       20.5       7.10       1.1696       710       11750       79300       2080       144655       20263       154       13       526         14T       21.5       6.70 <td< td=""></td<>
ICWW       24.5       8.18       1.0259       440       1366       11100       300       19795       3072       154       6       62.1         13Ts       24.0       6.60       1.1568       720       10130       77300       1940       138964       17260       135       18       486         13Td       22.0       6.80       1.1513       720       9740       77700       1860       90000         16       421         Day1       29.5*        1.1048       1450       6470       48400       1500       88150       12420        24       313         Day2       29.5       7.50       1.1248       1170       8600       59500       1730       109099       15205       266       28       382         12T       20.5       7.10       1.1696       710       11750       79300       2080       144655       20263       154       13       526         11T       21.5       6.70       1.1526       670       10650       74700       1870       134610       19619       79       13       455         14T       21.5       6.30
13Ts       24.0       6.60       1.1568       720       10130       77300       1940       138964       17260       135       18       486         13Td       22.0       6.80       1.1513       720       9740       77700       1860       90000         16       421         Day1       29.5*        1.1048       1450       6470       48400       1500       88150       12420        24       313         Day2       29.5       7.50       1.1248       1170       8600       59500       1730       109099       15205       266       28       382         12T       20.5       7.10       1.1696       710       11750       79300       2080       144655       20263       154       13       526         11T       21.5       6.70       1.1526       670       10650       74700       1870       134610       19619       79       13       455         14T       21.5       6.30       1.1704       570       12200       77100       2110       143799       18333       89       11       535
13Td       22.0       6.80       1.1513       720       9740       77700       1860       90000         16       421         Dayl       29.5*        1.1048       1450       6470       48400       1500       88150       12420        24       313         Dayl       29.5       7.50       1.1248       1170       8600       59500       1730       109099       15205       266       28       382         12T       20.5       7.10       1.1696       710       11750       79300       2080       144655       20263       154       13       526         11T       21.5       6.70       1.1526       670       10650       74700       1870       134610       19619       79       13       455         14T       21.5       6.30       1.1704       570       12200       77100       2110       143799       18333       89       11       535
Dayl 29.5* 1.1048 1450 6470 48400 1500 88150 12420 24 313  Dayl 29.5 7.50 1.1248 1170 8600 59500 1730 109099 15205 266 28 382  12T 20.5 7.10 1.1696 710 11750 79300 2080 144655 20263 154 13 526  11T 21.5 6.70 1.1526 670 10650 74700 1870 134610 19619 79 13 455  14T 21.5 6.30 1.1704 570 12200 77100 2110 143799 18333 89 11 535
Day2       29.5       7.50       1.1248       1170       8600       59500       1730       109099       15205       266       28       382         12T       20.5       7.10       1.1696       710       11750       79300       2080       144655       20263       154       13       526         11T       21.5       6.70       1.1526       670       10650       74700       1870       134610       19619       79       13       455         14T       21.5       6.30       1.1704       570       12200       77100       2110       143799       18333       89       11       535
12T       20.5       7.10 1.1696       710 11750 79300 2080 144655 20263 154 13 526         11T       21.5       6.70 1.1526       670 10650 74700 1870 134610 19619 79 13 455         14T       21.5       6.30 1.1704       570 12200 77100 2110 143799 18333 89 11 535
11T 21.5 6.70 1.1526 670 10650 74700 1870 134610 19619 79 13 455 14T 21.5 6.30 1.1704 570 12200 77100 2110 143799 18333 89 11 535
14T 21.5 6.30 1.1704 570 12200 77100 2110 143799 18333 89 11 535
15T 21.5 6.40 1.1713 540 12280 76100 2170 140605 20906 98 11 532
16T 21.9 6.50 1.1733 560 11940 81600 2280 150157 18333 79 11 555
17T 21.0 6.60 1.1417 990 7390 72800 2200 128861 11684 137 17 463
18T 21.0 6.90 1.0792 940 4460 36100 1100 65632 7610 154 21 242
9S 23.0 6.70 1.1161 1040 6970 54700 1470 98048 13037 317 19 355
8S 23.0 7.50 1.1156 1080 6920 53700 1360 96937 12245 280 19 362
AMLS 23.0 6.95 1.1122 960 7210 49500 1450 89730 14418 177 18 303
7S 23.0* 7.20 1.1152 920 6450 55500 1480 100130 9668 175 19 375
6S 23.9 6.80 1.1343 1110 7770 66600 1690 120586 11055 200 22 442
5S 24.0 7.00 1.1438 880 9150 71200 1990 128074 15812 172 20 452
4S 23.0 6.60 1.1277 1050 7470 60000 1500 109091 11254 228 22 410
3S 23.0 6.60 1.1309 960 7970 60000 1610 108602 13830 205 19 408
138 23.0 7.20 1.1513 750 9100 73700 2090 131197 16407 186 13 468
12S 21.0 7.35 1.1791 520 12660 82400 2380 151006 21560 261 9 555
11S 22.0 6.98 1.1725 530 11840 78100 2270 142094 21361 182 11 529

-106-March Analysis (continued)

Well	Temp	pН	density	7 Ca	Mg	Na	K	C1	so <sub>4</sub>	HCO.	Sr	Вr
									·			
14S	21.5	6.70	1.1772	510	11830	81000	2470	147606	20172	103	8	555
15S	21.5	7.00	1.1830	500	12470	83900	2620	153990	20172	228	9	581
1 6S	21.5	6.70	1.1892	450	12040	88800	2730	160396	20172	70	8	593
175	21.0	<b>6.9</b> 0	1.1616	560	9130	80800	2510	144205	13830	144	12	516
18S	21.0	6.65	1.0824	840	5200	42200	1280	76545	8479	149	44	275
9D	23.0	6.45	1.1115	940	6800	<b>538</b> 00	1410	96366	12486	290	17	329
8D	23.0	7.25	1.1190	1210	7840	54800	1380	101801	11906	303	15	359
AM1D	23.0	6.52	1.1311	780	8690	61700	1760	111836	15577	233	16	380
7D	23.2	7.39	1.1312	1010	7790	61900	1760	112490	12100	238	22	411
6D	24.0	6.75	1.1311	1040	8080	6300	1580	114322	12872	289	21	403
5D	23.5	6.55	1.1465	860	8830	70300	1970	126965	14032	256	21	474
4D	23.0	6.60	1.1312	1070	7990	61100	1520	111427	12486	266	23	351
3D	23.0*	6.45	1.0763	720	4760	<b>339</b> 00	870	61250			12	221
2D	23.0	6.48	1.0871	1210	5290	<b>392</b> 00	1030	71390	9974	347	16	270
13D	22.5	6.50	1.1497	860	8670	71100	2000	127962	13838	154	18	458
12D	21.0	6.95	1.1800	490	13660	84600	2440	157703	20988	322	11	560
11D	21.8	6.88	1.1739	510	11860	81700	2500	148519	20488	186	10	532
14D	21.8	6.35	1.1716	490	11630	80600	2290	146318	20022	103	9	528
1 5D	21.5	6.90	1.1845	500	11740	88900	2640	160102	19442	275	9	574
16D	21.5	6.60	1.1900	480	11800	91000	2720	163093	20215	83	8	631
17D	20.8	6.80	1.1723	560	10560	83500	2600	149494	18089	117	9	543
18D	21.0	7.10	1.0951	810	5240	45000	1330	8071 <b>9</b>	8814	158	45	294

\*Field temperature and therefore field density estimated

14T August analysis performed on non-acidified formaldehyde treated sample.

Appendix E

Hydrology

APPENDIX E Determining the piezometric potential

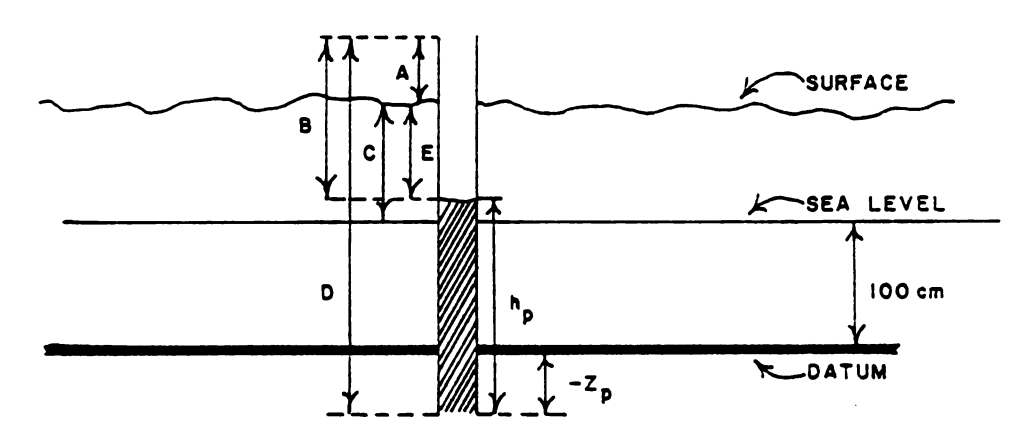
A - height of well pipe above the ground (weasured)

B - depth from top of well pipe to water (measured)

C - land elevation with sea level as reference (measured)

D - length of well pipe (measured)

 $\boldsymbol{\Xi}$  - level of water in well pipe with land elevation as reference (measured)



## EXAMPLE 1 Well 6 shallow for August 1979

A = 15.24 cm

 $D - B = 190.0 - 55.88 = 134.12 = h_p$ 

B = 55.88 cm

D - (A + C + 100 cm) =

C = 19.20 cm

 $190.0 - (15.24 + 48.79 + 100) = 25.97 = -Z_p$ 

D = 74.80 cm Density = DEN = 1.1353

Piezometric potential =  $\emptyset$  = DEN(n<sub>p</sub> + Z<sub>p</sub>) = 1.1353(134.12 - 25.97)

## EXAMPLE 2: Seawater

 $h_p = 100 \text{ cm}$ 

 $z_p = 0.0$ 

DEN = 1.023

Piezometric potential =  $\emptyset$  = 1.023(100 + 0.0) = 102.3